currents. In addition, flecainide inhibited I_A, but it preferentially inhibited TEA-insensitive I_A with an IC_{50} of 30 M in comparison with TEA-sensitive I_A. I_A formed by K_V4 currents has been reported to be more sensitive to inhibition by flecainide ($IC_{50}<20\,\mu M$) (Yamashita *et al.*, 1995; Yeola & Snyders, 1997), suggesting that $K_V3.4$ current is resistant to flecainide compared with K_V4 currents, and I_A in cultured hPASMCs is composed of these two different types of channels.

Two components of I_A could also be distinguished by the kinetic properties of the channels (voltage of half inactivation and time courses of recovery from inactivation). Based on the expression system of $K_V3.4$ and K_V4 ($K_V4.1$, $K_V4.2$, $K_V4.3$) (Pak *et al.*, 1991; Schroter *et al.*, 1991; Coetzee *et al.*, 1999), $K_V3.4$ and K_V4 have the mean voltages at half inactivation of -20 to -32 mV and -50 to 69 mV, and K_V4 shows the fast recovery from inactivation compared with $K_V3.4$, which are consistent with our proposal that I_A consists of two different types of I_A, $K_V3.4$ and K_V4.

RT–PCR analysis identified the I_A-related genes (Baldwin *et al.*, 1991; Pak *et al.*, 1991; Rudy *et al.*, 1991; Schroter *et al.*, 1991) encoding for $K_V3.4$, $K_V4.1$, $K_V4.2$ and $K_V4.3$, but not $K_V1.4$ or $K_V3.3$, irrespective of passage numbers (3 and 8). The detailed quantitative real-time RT–PCR analysis provided evidence that the relative abundance of I_A-encoding α-subunit expression was $K_V4.2>K_V3.4>K_V4.3$ (long)$>K_V4.1$ with a ratio of 1.00 : 0.55 : 0.20 : 0.09. K_V1 coexpressed with accessory β-subunits can also form I_A (Rettig *et al.*, 1994; Heinemann *et al.*, 1996). However, DTX, a blocker of $K_V1.1$ and $K_V1.2$, CTX, a blocker of $K_V1.2$ and $K_V1.3$ (Grissmer *et al.*, 1994) and clofilium, a blocker of $K_V1.5$ (Malayev *et al.*, 1995), did not inhibit I_A. Therefore, the channel of K_V1 does not seem to be involved in forming I_A in hPASMCs. These observations suggest that I_A consists of two different types of I_A, $K_V3.4$ and K_V4. RT–PCR has shown the presence of $K_V3.4$, $K_V4.1$, $K_V4.2$ and $K_V4.3$ mRNA in rat PASMCs (Yuan XJ *et al.*, 1998; Davies & Kozlowski, 2001; Platoshyn *et al.*, 2001; Yuan, 2001), but the present study provided the direct evidence in cultured hPASMCs based on electrophysiological and molecular analyses. The immunocytochemical findings of $K_V3.4$ corresponded well with the results of RT–PCR. The presence of $K_V3.4$ was also confirmed by the immunohistochemical studies using intact hPA sections of the main and small PA. RT–PCR also showed the presence of $K_V4.1$, $K_V4.2$ and $K_V4.3$ mRNA, and the real-time RT–PCR analysis clearly provided the evidence showing that the relative abundance of K_V was $K_V4.2>K_V4.3$ (long)$>K_V4.1$. In this study, we showed that transcripts encoding $K_V4.2$ and $K_V4.3$ were 11- and two-fold more abundant than $K_V4.1$ transcripts, respectively. The immunocytochemical findings also showed that $K_V4.2$ and $K_V4.3$ were expressed in cultured hPASMCs, and in intact hPA sections. We could not rule out the possible involvement of $K_V4.1$ on I_A, because anti-$K_V4.1$ antibody was not commercially available. Further studies are needed to clarify this possibility, but K_V4 is likely to be the major component of TEA-insensitive I_A in cultured hPASMCs. KChIPs, which interact with the NH_2 terminus of K_V4 proteins, enhance surface expression and modulate the kinetics of the channels (An *et al.*, 2000, Bahring *et al.*, 2001). It has been reported that KChIP1 is predominant in murine colonic myocytes (Amberg *et al.*, 2002) and KChIP1 and KChIP3 are extensively expressed in mouse gastrointestinal myocytes (Ohya & Horowitz, 2002). The present study showed that KChIP expressed in cultured hPASMCs is mainly composed of KChIP3. From these observations, we conclude that K_V4, in association with KChIP3, is the major molecular determinant of I_A in cultured hPASMCs.

The functions of I_A in hPASMCs remain unsettled. Both components of I_A (K_V4 and $K_V3.4$ currents) were activated at potentials more positive than -40 mV, which suggests that it may not play an important role in forming membrane potential in hPASMCs. Instead, it is likely that I_A inhibits membrane excitability and prevents depolarizing stimuli such as hypoxia under the pathophysiological conditions (Osipenko *et al.*, 1997; Turner & Kozlowski, 1997; Archer *et al.*, 1998; Patel & Honore, 2001; Gurney *et al.*, 2003). In addition, $K_V3.4$ appears to be modulated by oxidant stress (Serodio *et al.*, 1994; Duprat *et al.*, 1995), proposing that $K_V3.4$ may play a modulatory role in excitability of hPASMCs under the various pathophysiological conditions such as hypoxia. However, further studies are needed to clarify the physiological significance of I_A in hPASMCs.

In conclusion, I_A in cultured hPASMCs consists of two kinetically and pharmacologically distinct components, possibly $K_V3.4$ and K_V4 plus KChIP3.

Limitations of our study

The present study used cultured hPASMCs instead of freshly isolated cells because it is difficult for us to obtain human tissues. The presence of a heterogeneous population of smooth muscle cells in the PA has been reported (Smirnov *et al.*, 2002), but expression of $K_V3.4$ and K_V4 was detected in cultured hPASMCs irrespective of passage number, and was confirmed by immunohistochemical analysis using PA preparations. Therefore, the findings obtained from the present study are likely to hold in native human PA, but further studies using freshly isolated hPASMCs are needed.

References

AMBERG, G.C., KOH, S.D., IMAIZUMI, Y., OHYA, S. & SANDERS, K.M. (2002). A-type potassium currents in smooth muscle. *Am. J. Physiol.*, **284**, C583–C595.

AN, W.F., BOWLBY, M.R., BETTY, M., CAO, J., LING, H.P., MENDOZA, G., HINSON, J.W., MATTSON, K.I., STRASSLE, B.W., TRIMMER, J.S. & RHODES, K.J. (2000). Modulation of A-type potassium channels by a family of calcium sensors. *Nature*, **403**, 553–556.

ARCHER, S.L., SOUIL, E., DINH-XUAN, A.T., SCHREMMER, B., MERCIER, J.C., YAAGOUBI, A., NGUYEN-HUU, L., REEVE, H.L. & HAMPL, V. (1998). Molecular identification of the role of voltage-gated K^+ channels, $K_V1.5$ and $K_V2.1$ in hypoxic pulmonary vasoconstriction and control of resting membrane potential in rat pulmonary artery myocytes. *J. Clin. Invest.*, **101**, 2319–2330.

BAHRING, R., DANNENGERG, J., PETERS, H.C., LEICHER, T., PONGS, O. & ISBRANDT, D. (2001). Conserved K_V4 N-terminal domain critical for effects of K_V channel-interacting protein 2.2 on channel expression and gating. *J. Biol.Chem.*, **276**, 23888–23894.

BALDWIN, T.J., TSAUR, M.L., LOPEZ, G.A., JAN, Y.N. & JAN, L.Y. (1991). Characterization of a mammalian cDNA from an inactivating voltage-sensitive K^+ channel. *Neuron*, **7**, 471–483.

CHAGOT, B., ESCOUBAS, P., VILLEGAS, E., BERNARD, C., FERRAT, G., CORZO, G., LAZDUNSKI, M. & DARBAN, H. (2004). Solution structure of Phrixotoxin-1, a specific peptide inhibitor of K_V4 potassium channels from the venom of the theraphoid spider *Phrixotrichus auratus*. *Protein Sci.*, **13,** 1197–1208.

CLAPP, L.H. & GURNEY, A.M. (1991). Outward currents in rabbit pulmonary artery cells dissociated with a new technique. *Exp. Physiol.*, **76,** 677–693.

COETZEE, W.A., AMARILLO, Y., CHIU, J., CHOW, A., LAU, D., MECORMACK, T., MORENO, H., NADAL, M.C., OZAITA, A., POUNTNEY, D., SAGANICH, M., VEGA-SAENY DE MIERA, E. & RUDY, B. (1999). Molecular diversity of K^+ channels. *Ann. N. Acad. Sci.*, **868,** 233–285.

COPPOCK, E.A. & TAMKUN, M.M. (2001). Differential expression of K(V) channel alpha- and beta-subunits in the bovine pulmonary arterial circulation. *Am. J. Physiol.*, **281,** L1350–L1360.

DAVIES, A.R. & KOZLOWSKI, R.Z. (2001). Kv channel subunit expression in rat pulmonary arteries. *Lung*, **179,** 147–161.

DIOCHOT, S., SCHWEITZ, H., BERESS, L. & LAZDUNSKI, M. (1998). Sea anemone peptides with a specific blocking activity against the fast inactivating potassium channel $K_V3.4$. *J. Biol. Chem.*, **273,** 6744–6749.

DUPRAT, F., GUILLEMARE, E., ROMEY, G., FINK, M., LESAGE F LAZDUNSKI, M. & HONORE, E. (1995). Susceptibility of cloned K^+ channels to reactive oxygen species. *Proc. Natl. Acad. Sci. U.S.A.*, **92,** 11796–11800.

GRISSMER, S., NGUYEN, A.N., AIYAR, J., HANSON, D.C., MATHER, R.J., GUTMAN, G.A., KARMILOWICZ, M.J., AUPERIN, D.P. & CHANDY, K.G. (1994). Pharmacological characterization of five cloned voltage-gated K^+ channels, types $K_V1.1$, 1.2, 1.3, 1.5, and 3.1, stably expressed in mammalian cell lines. *Mol. Pharmacol.*, **45,** 1227–1234.

GURNEY, A.M., OSIENKO, O.N., MACMILLIAN, D., MCFARLANE, K.M., TATE, R.J. & KEMPSILL, F.E.J. (2003). Two-pore domain K channel, TASK-1, in pulmonary artery smooth muscle cells. *Circ. Res.*, **93,** 957–964.

HAMILL, O.P., MARTY, A., NEHER, E., SAKMANN, B. & SIGWORTH, F.J. (1981). Improved patch-clamp techniques for high-resolution current recording from cells and cell-free membrane patches. *Pflug. Arch.*, **391,** 85–100.

HEINEMANN, S.H., RETTIG, J., GRAACK, H.R. & PONGS, O. (1996). Functional characterization of K_V channel β-subunits from rat brain. *J. Physiol.*, **493,** 625–633.

HULME, J.T., COPPOCK, E.A., FELIPE, A., MARTENS, J.R. & TAMKUM, M.M. (1999). Oxygen sensitivity of cloned voltage-gated K^+ channels expressed in the pulmonary vasculature. *Circ. Res.*, **85,** 489–497.

JAMES, A.F., OKADA, T. & HORIE, M. (1995). A fast transient outward current in cultured cells from human pulmonary artery smooth muscle. *Am. J. Physiol.*, **268,** H2358–H2365.

MALAYEV, A.A., NELSON, D.J. & PHILIPSON, L.H. (1995). Mechanism of clofilium block of the human $K_V1.5$ delayed rectifier potassium channel. *Mol. Pharmacol.*, **47,** 198–205.

NAKAJIMA, T., IWASAWA, K., OONUMA, H., IMUTA, H., HAZAMA, H., ASANO, M., MORITA, T., NAKAMURA, F., SUZUKI, J., SUZUKI, S., KAWAKAMI, Y., OMATA, M. & OKUDA, Y. (1999). Troglitazone inhibits voltage-dependent calcium currents in guinea pig cardiac myocytes. *Circulation*, **99,** 2942–2950.

NELSON, M.T. & QUAYLE, J.M. (1995). Physiological roles and properties of potassium channels in arterial smooth muscle. *Am. J. Physiol.*, **268,** C799–C822.

OHYA, S. & HOROWITZ, B. (2002). Differential transcriptional expression of Ca^{2+} BP superfamilies in murine gastrointestinal smooth muscles. *Am. J. Physiol.*, **283,** G1290–G1297.

OHYA, S., TANAKA, M., OKU, T., ASAI, Y., WATANABE, M., GILES, W.R. & IMAIZUMI, Y. (1997). Molecular cloning and tissue distribution of an alternatively spliced variant of an A-type K^+ channel α-subunit, $K_V4.3$ in the rat. *FEBS Lett.*, **420,** 47–53.

OKABE, K., KITAMURA, K. & KURIYAMA, H. (1987). Features of 4-aminopyridine sensitive outward current observed in single smooth muscle cells from the rabbit pulmonary artery. *Pflugers Arch.*, **409,** 561–568.

OONUMA, H., IWASAWA, K., IIDA, H., NAGATA, T., IMUTA, H., MORITA, Y., YAMAMOTO, K., NAGAI, R., OMATA, M. & NAKAJIMA, T. (2002). Inward rectifier K^+ current in human bronchial smooth muscle cells: inhibition with antisense oligonucleotides targeted to Kir2.1 mRNA. *Am. J. Resp. Cell. Mol. Biol.*, **26,** 371–379.

OSIPENKO, O.N., EVANS, A.M. & GURNEY, A.M. (1997). Regulation of the resting potential of rabbit pulmonary artery myocytes by a low threshold, O_2-sensing potassium current. *Br. J. Pharmacol.*, **120,** 1461–1470.

PAK, M.D., BAKER, K., COVARRUBIAS, M., BUTLER, A., RATCLIFFE, A. & SALKOFF, L. (1991). mShal, a subfamily of A-type K^+ channel cloned from mammalian brain. *Proc. Natl. Acad. Sci. U.S.A.*, **88,** 4386–4390.

PATEL, A.J. & HONORE, E. (2001). Molecular physiology of oxgen-sensitive potassium channels. *Eur. Respir. J.*, **18,** 221–227.

PATEL, A.J., LAZDUNSKI, M. & HONORE, E. (1997). $K_V2.1/K_V9.3$, a novel ATP-dependent delayed rectifier K^+ channel in oxygen-sensitive pulmonary artery myocytes. *EMBO J.*, **16,** 6615–6625.

PEREZ-GARCIA, M.T., LOPEZ-LPPEZ, J.R., RIESCO, A.M., HOPPE, U.C., MARBAN, E., GONZALEZ, C. & JOHNS, D.C. (2000). Viral gene transfer of dominant-negative K_V4 construct suppresses an O_2-sensitive K^+ current in chemoreceptor cells. *J. Neurosci.*, **20,** 5689–5695.

PLATOSHYN, O., YU, Y., GOLOVINA, V.A., MCDANIEL, S.S., KRICK, S., LI, L., WANG, J.Y., RUBIN, L.J. & YUAN, J.X. (2001). Chronic hypoxia decreases K(V) channel expression and function in pulmonary artery myocytes. *Am. J. Physiol.*, **280,** L801–L812.

RETTIG, J., HEINEMANN, S.H., WUNDER, F., LORRA, C., PARCEI, D.N., DOLLY, J.O. & PONGS, O. (1994). Inactivation properties of voltage-gated K^+ channels altered by presence of β-subunit. *Nature*, **369,** 289–294.

RUDY, B., SEN, K., VEGA-SAENZ DE MIERA, E., LAU, D., RIED, T. & WARD, D.C. (1991). Cloning of a human cDNA expressing a high voltage-activating, TEA-sensitive, type-A K^+ channel which maps to chromosome 1 band p21. *J. Neurosci. Res.*, **29,** 401–412.

SCHROTER, K.H., RUPPERSBERG, J.P., WUNDER, F., RETTIG, J., STOCKER, M. & PONGS, O. (1991). Cloning and functional expression of a TEA-sensitive A-type potassium channel from rat brain. *FEBS Lett.*, **278,** 211–216.

SERODIO, P., KENTROS, C. & Rudy, B. (1994). Identification of molecular components of A-type channels activating at subthreshold potentials. *J. Neurosci.*, **72,** 1516–1529.

SMIRNOV, S.V., BECK, R., TAMMARÓ, P., ISHII, T. & AARONSON, P.I. (2002). Electorophysiologically distinct smooth muscle cell subtypes in rat conduit and resistance pulmonary arteries. *J. Physiol.*, **538,** 867–878.

STUHMER, W., RUPPERSBERG, J.P., SCHROTER, K.H., SAKMANN, B., STOCKER, M., GIESE, K.P., PERSCHKE, A., BAUMANN, A. & PONGS, O. (1998). Molecular basis of functional diversity of voltage-gated potassium channels in mammalian brain. *EMBO. J.*, **8,** 3235–3244.

TERASAWA, K., NAKAJIMA, T., IIDA, H., IWASAWA, K., OONUMA, H., JO, T., NAKAMURA, F., FUJIMORI, Y., TOYO-OKA, T. & NAGAI, R. (2002). Nonselective cation currents regulate membrane potential of rabbit coronary arterial cell: modulation by lysophoshatidylcholine. *Circulation*, **106,** 3111–3119.

TURNER, J.L. & KOZLOWSKI, R.Z. (1997). Relationship between membrane potential, delayed rectifier K^+ currents and hypoxia in rat pulmonary arterial myocytes. *Exp. Physiol.*, **82,** 629–645.

WANG, I., JUHASZOVA, M., CONTE, J.V., GAINE, S.P., RUBIN, L.J. & YUAN, J.X. (1998). Action of fenfluramine on voltage-gated K^+ channels in human pulmonary artery smooth muscle cells [letter]. *Lancet*, **352,** 290.

WEIR, E.K., REEVE, H.L., HUANG, J.M., MICHELAKIS, E., NELSON, D.P., HAMPAL, V. & ARCHER, S.L. (1996). Anorexic agents, aminorex, fenfluramine, and dexfenfluramine inhibit potassium current in rat pulmonary vascular smooth muscle and cause pulmonary vasoconstriction. *Circulation*, **94,** 2216–2220.

YAMASHITA, T., NAKAJIMA, T., HAMADA, E., HAZAMA, H., OMATA, M. & KURACHI, Y. (1995). Flecainide inhibits the transient outward current in atrial myocytes isolated from the rabbit heart. *J. Pharmacol. Exp. Ther.*, **274,** 315–321.

YEOLA, S.W. & SNYDERS, D.J. (1997). Electrophysiological and pharmacological correspondence between $K_V4.2$ current and rat cardiac transient outward current. *Cardiovasc. Res.*, **33,** 540–547.

YUAN, J.X. (2001). Oxygen-sensitive K^+ channels: where and what? *Am. J. Physiol.*, **281,** L1345–L1349.

YUAN, J.X., ALDINGER, A.M., JUHASZOVA, M., WANG, J., CONTE JR, J.V., GAINE, S.P., ORENS, J.B. & RUBIN, L.J. (1998). Dysfunctional voltage-gated K^+ channels in pulmonary artery smooth muscle cells of patients with primary pulmonary hypertension. *Circulation*, **98**, 1400–1406.

YUAN, X.J. (1995). Voltage-gated K^+ currents regulate resting membrane potential and $[Ca^{2+}]_i$ in pulmonary arterial myocytes. *Circ. Res.*, **77**, 370–378.

YUAN, X.J., GOLDMAN, W.F., TOD, M.L., RUBIN, L.J. & BLAUSTEIN, M.P. (1993). Ionic currents in rat pulmonary and mesenteric arterial myocytes in primary culture and subculture. *Am. J. Physiol.*, **264**, L107–L115.

YUAN, X.J., WANG, J., JUHASZOVA, M., GOLOVINA, V.A. & RUBIN, L.J. (1998). Molecular basis and function of voltage-gated K^+ channels in pulmonary arterial smooth muscle cells. *Am. J. Physiol.*, **274**, L621–L635.

(Received October 26, 2004
Revised March 17, 2005
Accepted April 22, 2005
Published online 6 June 2005)

Journal of General Virology (2004), 85, 2209–2214 DOI 10.1099/vir.0.79940-0

Short Communication

The adenovirus E1A and E1B19K genes provide a helper function for transfection-based adeno-associated virus vector production

Takashi Matsushita,[1] Takashi Okada,[1] Toshiya Inaba,[2] Hiroaki Mizukami,[1] Keiya Ozawa[1] and Peter Colosi[3]

[1]Division of Genetic Therapeutics, Center for Molecular Medicine, Jichi Medical School, 3311-1 Yakushiji, Minami-kawachi, Kawachi, Tochigi 329-0489, Japan

[2]Department of Molecular Oncology, Research Institute for Radiation Biology and Medicine, Hiroshima University, Hiroshima 734-8553, Japan

[3]Avigen Inc., Alameda, CA, USA

Correspondence
Takashi Okada
tokada@jichi.ac.jp
Peter Colosi
PColosi@avigen.com

Received 26 December 2003
Accepted 17 May 2004

Although the adenoviral E1, E2A, E4 and VA RNA regions are required for efficient adeno-associated virus (AAV) vector production, the role that the individual E1 genes (*E1A*, *E1B19K*, *E1B55K* and *protein IX*) play in AAV vector production has not been clearly determined. E1 mutants were analysed for their ability to mediate AAV vector production in HeLa or KB cells, when cotransfected with plasmids encoding all other packaging functions. Disruption of *E1A* and *E1B19K* genes resulted in vector yield reduction by up to 10- and 100-fold, respectively, relative to the wild-type E1. Interruption of the *E1B55K* and *protein IX* genes had a modest effect on vector production. Interestingly, expression of anti-apoptotic E1B19K cellular homologues such as Bcl-2 or Bcl-x_L fully complemented E1B19K mutants for AAV vector production. These findings may be valuable for the future development of packaging cell lines for AAV vector production.

Adeno-associated virus (AAV)-based vector systems are particularly attractive vehicles for clinical applications requiring long-term *in vivo* gene expression from post-mitotic tissues. AAV vectors have been shown to promote stable expression of a wide variety of transgenes in numerous tissues, including skeletal and cardiac muscle, liver, the central nervous system and retina (Rabinowitz & Samulski, 1998). Overt evidence of inflammation is either minimal or non-existent in target tissues immediately following AAV vector administration. Furthermore, cytotoxic T-lymphocyte responses are not normally elicited to transgene products delivered by AAV vectors, even when such proteins are foreign to the host (Jooss *et al.*, 1998). AAV vectors are considered to be relatively safe because the parental virus is non-pathogenic and unable to replicate in the absence of a co-infecting helper virus. Additionally, current production methods have reduced the regeneration of replication competent wild-type AAV during vector production to undetectable levels (Allen *et al.*, 1997). Finally, the robust protein capsid of AAV makes AAV vectors particularly amenable to existing production methods for protein pharmaceuticals (Gao *et al.*, 2000) and confers upon them desirable drug stability characteristics.

AAV2, the parent virus from which the vector system is derived, is replication defective and requires co-infection of helper viruses to propagate. Adenovirus (Atchinson *et al.*, 1965) and herpes virus (Buller *et al.*, 1981) act as complete helpers and vaccinia virus (Schlehofer *et al.*, 1986) acts as a partial helper. The set of adenoviral (type 2 or 5) genes that facilitate AAV2 propagation has been defined and consists of E1A, E1B55K, the VA RNAs, E2A and E4orf6 (Samulski & Shenk, 1988). E1A acts as a cue to begin virus replication by up-regulating transcription from the *rep* gene promoters, P5 and P19 (Tratschin *et al.*, 1984) and by activating the early adenovirus promoters. E1A is also required to drive the host cell into the S-phase of the cell cycle for viral DNA replication because the AAV encoded proteins are not capable of this function. An adverse effect of E1A is that it stabilizes p53, which leads to apoptosis (Lowe *et al.*, 1993). To prevent this, the E1B55K and the E4orf6 proteins form a complex with p53 and cause it to be degraded through ubiquitin-mediated proteolysis (Querido *et al.*, 1997; Steegenga *et al.*, 1998). Later in infection, E1B55K and E4orf6 form a heterodimer that causes the preferential export of AAV and adenoviral late mRNAs from the nucleus while inhibiting the transit of adenoviral early and cellular mRNAs (Pilder *et al.*, 1986). The 72 kDa DNA-binding protein encoded by E2A has functions in viral DNA replication, viral mRNA processing and export, and AAV promoter regulation (Carter *et al.*, 1992; Ward *et al.*, 1998; Chang & Shenk, 1990). It causes an increase in the intracellular levels of the

single- and double-stranded forms of the AAV genome, the spliced forms of the rep proteins, and dramatically increases capsid protein production. Lastly, the VA RNAs inhibit the interferon-inducible eIF-2 protein kinase, thereby circumventing this cellular anti-viral mechanism from blocking viral protein translation (West *et al.*, 1987).

With respect to E2A, E4orf6 and the VA RNAs, the helper gene requirement for AAV vector and virus production is identical. We and others, have shown that plasmids encoding these genes, when cotransfected into 293 cells along with plasmids encoding rep/cap and a vector, mediate higher levels of vector production than that produced by adenovirus infection (Xiao *et al.*, 1998; Matsushita *et al.*, 1998). This so-called 'triple plasmid' transfection method forms the basis of the current scale-up vector production effort at Avigen and has a respectable mean production efficiency of 1×10^{13} vector genomes produced per 850 cm^2 roller bottle. A report was published describing a method for producing AAV vector in 293 cells using only E4orf6 as the helper gene (Allen *et al.*, 2000). This method requires the use of a heterologous promoter to drive the capsid gene and is about 10-fold less productive than methods using a plasmid encoding all three adenoviral helper genes (unpublished data).

The genes of the E1 region have not been analysed for their contribution to AAV vector production. In this study, we have investigated the role of the *E1A* and *E1B* genes in AAV vector production by using a series of E1 mutant plasmids and cell lines that lack adenoviral genes. E1A was required for efficient vector production. In contrast to the helper requirements for AAV production, our data indicated that *E1B19K* gene greatly augmented vector production, however, *E1B55K* gene did not.

The contributions of each of the component genes from the E1 region to AAV helper function was assessed by creating a set of plasmids with mutations in the *E1A*, *E1B19K*, *E1B55K* or *protein IX* genes and then testing them for their ability to support transfection-based AAV vector production. At least one truncation or one deletion mutation was made for each gene (Fig. 1).

For vector construction the plasmid pE1, which encodes the *E1A*, *E1B19K*, *E1B55K* and *protein IX* genes, was created from Ad2 DNA (Invitrogen). Briefly, the *Afl*III fragment (nt positions 142–5927) of Ad2 was cloned into the *Afl*III site of pBR322 (New England Biolabs) to generate pE1. pE1A-825stop was constructed by the insertion of an adapter (CCGGACTAATTAACTAGT), which includes a stop codon and an *Spe*I site, into the *Bsp*EI site of pE1. Similarly, pE1B19K-1912stop, pE1B55K-2243stop,

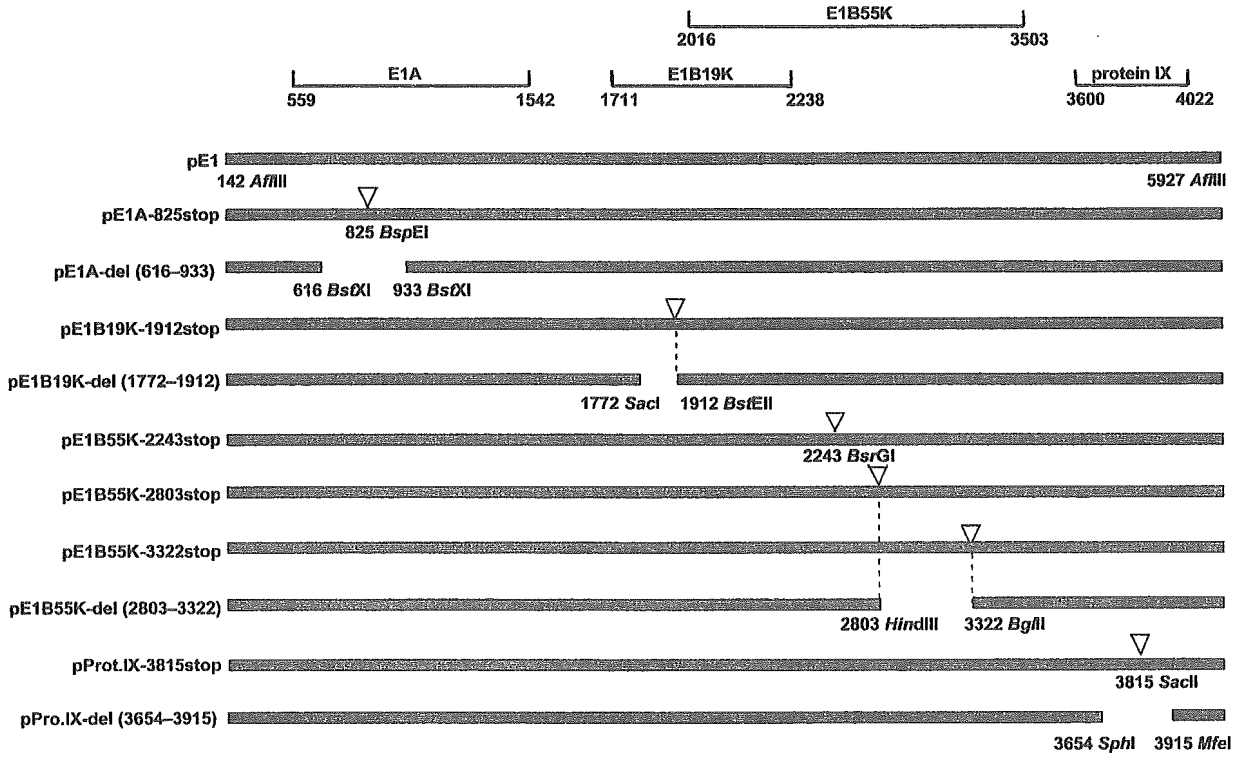

Fig. 1. Schematic representation of plasmids harbouring adenoviral E1 mutants used in this study. A 5·8 kb DNA fragment of adenovirus type 2 was cloned into the *Afl*III site of pBR322. pE1 encodes the entire E1 region, and the E1 mutant plasmids shown here were derived from it. The vertical flags mark the positions of inserted stop codons. The gaps in pE1A, pE1B19K, pE1B55K or pProt.IX constructs represent deletions.

pE1B55K-2803stop and pE1B55K-3322stop were made by the insertion of oligonucleotides into the *Bst*EII, *Bsr*GI, *Hin*dIII and *Bgl*II sites of pE1, respectively. pE1A-del (616–933) has a deletion of a 318 bp segment (positions 616–933 in Ad2). pE1B19K-del (1772–1912) and pE1B55K-del (2803–3322) have the same deletions as *dl337* (Pilder *et al.*, 1984) and *dl338* (Pilder *et al.*, 1986), respectively, used by Samulski & Shenk (1988) to examine E1 helper function for AAV2 production. Briefly, pE1B19K-del (1772–1912) lacks sequences between positions 1772 and 1912, and pE1B55K-del (2803–3322) lacks sequences between positions 2803 and 3322. pProt.IX-3815stop was constructed by the insertion of oligonucleotides into a *Sac*II site. pProt.IX-del (3654–3915) lacks a 262 bp segment (between positions 3654 and 3915 of Ad2).

The helper activities of the various E1 plasmids were assayed by cotransfecting them with a plasmid encoding both an AAV CMV*lacZ* vector and rep/cap (pW4389LacZ), and a plasmid encoding the adenovirus-2 VA RNA, E2A and E4 regions (Pladeno5), into KB or HeLa cells, and then quantifying *lacZ* vector production as described previously (Matsushita *et al.*, 1998). AAV vector was harvested 40 or 72 h after transfection and stocks were prepared by the freeze-thaw method. AAV vector production was quantified by titration of the vector stocks in 293 cells in the presence of adenovirus, followed by X-Gal staining and manual counting by light microscopy. For each experiment, all constructs were tested using triplicate production cultures, and all experiments were conducted at least three times, independently.

Elimination of the entire E1 region resulted in 2 (HeLa cells) to 3 log (KB cells) reduction in vector production relative to production in the presence of pE1, a plasmid encoding the entire E1 region ($P<0{\cdot}01$ by Student's *t*-test) (Fig. 2a, b). Disruption of the *E1A* genes, whether by truncation or deletion, caused 1 (HeLa cells) to 1·5 log (KB cells) reduction in vector production ($P<0{\cdot}01$). Truncations or deletions in the *E1B19K* gene also resulted in substantial reduction in vector production, 1 log in HeLa cells and greater than 2 logs in KB cells ($P<0{\cdot}01$). The lesser severity of the E1B19K mutant in HeLa cells, relative to KB cells, may be due to the relatively high level of Bcl-2 expression in HeLa cells (Liang *et al.*, 1995), or the human papilloma virus E6/E7 genes they harbour. The E6/E7 genes have been shown to facilitate some of the processes in AAV replication (Walz *et al.*, 1997). In most cases, disruption of the *E1B55K* and *protein IX* genes had a modest effect on vector production in either HeLa or KB cells. Two constructs, pE1B55K-2243stop and pProt.IX-3815stop showed fivefold reduction in vector yield in KB cells but little reduction in HeLa cells.

Our results differ substantially from those of Samulski & Shenk (1988) who examined the effect of E1B adenovirus mutants on AAV2 production, DNA replication, and mRNA and protein expression. This group found that an E1B19K adenovirus-2 mutant (*dl337*) mediated efficient AAV production from HeLa cells transfected with a plasmid encoding an AAV wild-type provirus (pSM620) but that

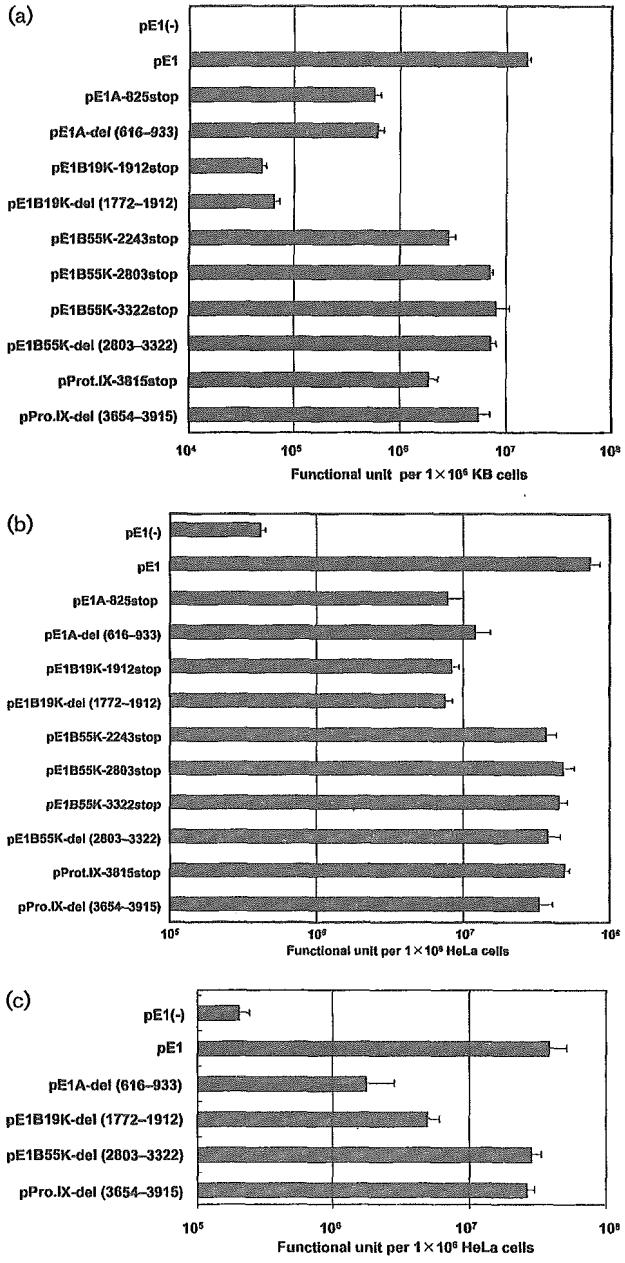

Fig. 2. Comparison of E1 mutant plasmids with respect to AAV helper function in KB (a) and HeLa cells (b) at 72 h after transfection, or in HeLa cells (c) at 40 h after the transfection. AAV *lacZ* vector was produced by the transfection of HeLa or KB cells with pW4389lacZ (encodes rep/cap and an AAV *lacZ* vector) and pladeno 5 (encodes the E2A, E4 and VA RNA regions), in the presence and absence of the indicated E1 plasmids. AAV vector production was assessed by titration of *lacZ* vector in 293 cells. pE1 (-) is identical to pBR322 without the expression cassette. Each bar represents the mean value obtained from triplicate cultures, and the error bar represents the standard deviation.

E1B55K (*dl338*) and E4orf6 (*dl355*) adenovirus mutants did not. AAV virion production was measured at a 40 h time point. The E1B55K and E4orf6 defects were caused by a delay in AAV mRNA accumulation that resulted in delays in viral DNA replication, capsid expression and ultimately virus production. AAV mRNA, DNA and capsid protein concentrations in cultures infected with E1B55K and E4orf6 mutants eventually reached levels seen in cultures infected by wild-type adenovirus but at longer time points, 72–96 h for adenovirus mutants compared with 24–40 h for wild-type adenovirus.

An important difference between our study and that of Samulski & Shenk (1988) was the timing of AAV/AAV vector harvest, 40 h in our study versus 72 h in theirs. Therefore, we examined a subset of the E1 region plasmids in transfection experiments using the same 40 h time point for vector harvest (Fig. 2c). The results were essentially similar to those at the 72 h time point and still differed from those produced by the adenovirus mutants. This observed difference in helper gene requirement may be attributable to technical factors associated with using virus infection or DNA transfection. A possible explanation for the conclusions reached by Samulski & Shenk (1988) might be the differences in the growth rates of the adenovirus mutants tested. The E1B55k mutant, *dl338*, was reported to grow inefficiently (100-fold reduced relative to wild-type) in HeLa cells (Pilder *et al.*, 1986) while the E1B19K mutant, *dl337*, was reported to be less defective (about 10-fold reduced relative to wild-type) (Pilder *et al.*, 1984). The lag in AAV mRNA, DNA and virus production seen with the E1B55K mutant may be simply because of a slow growing helper virus, resulting in low copy numbers of all of the adenovirus helper genes, and may not be directly due to the lack of the mutated gene. The observation that E1B19K is apparently not required for adenovirus mediated AAV production is harder to explain. It is tempting to speculate that the transfection-based production system benefits from additional anti-apoptitic activity provided by E1B19K. If this is true, this requirement does not appear to be cell-type or transfection-reagent specific (calcium phosphate and polycation-based transfection reagents both show an E1B19K effect, data not shown), and may have something to do with the adenoviral helper gene dose or kinetics of expression. Other differences between the two methods of identifying AAV helper function include: transfection method, the packaging of AAV virus versus a vector, and the use of replicating helper (AAV) versus non-replicating plasmid helpers. Full resolution of these issues will require further experimentation.

The adenovirus *E1B19K* gene, and its cellular homologues Bcl-2 and Bcl-x_L, encode anti-apoptotic proteins that function by inhibiting proapoptotic Bcl-2 homologues, such as Bax and Bak, by forming inactive heterodimers with them. To determine whether other anti-apoptotic members of the Bcl-2 family could augment AAV vector production, plasmid vectors expressing the *E1B19K*, *Bcl-2* or *Bcl-x_L* gene

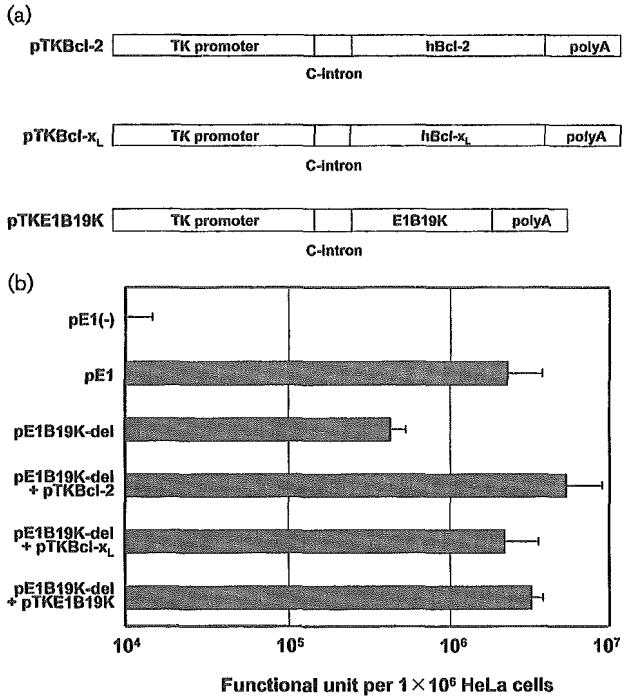

Fig. 3. (a) Schematic representation of Bcl-2, Bcl-x_L and E1B19K expression plasmids. TK promoter, HSV-*tk* promoter; C-intron, chimeric CMV/β-globin intron; polyA, SV40 late polyadenylation signal; hBcl-2, human Bcl-2 cDNA; hBcl-x_L, human Bcl-x_L cDNA; and E1B19K, adenovirus type 2 early region 1B 19 kDa protein gene. (b) Bcl-2 family members complement the vector production defect of an E1B19K mutant in HeLa cells. AAV *lacZ* vector was produced by the transfection of HeLa cells with pW4389lacZ (encodes rep/cap and an AAV *lacZ* vector), pladeno 5 (encodes the E2A, E4 and VA RNA regions), and pE1B19K-del (1772–1912), in the presence and absence of the indicated plasmids expressing Bcl-2 family genes, including E1B19K. AAV vector production was assessed by titration of *lacZ* vector in 293 cells. Each bar represents the mean value of triplicate cultures and the error bar represents the standard deviation.

products were tested for their ability to complement the vector production defect of the E1B19K deletion mutant, pE1B19K-del (1772–1912) (Fig. 3a). pTKPRMCS was assembled by the removal of a *Renilla* luciferase (R*luc*) reporter gene from pRL-TK (Promega) (between the *Nhe*I and *Xba*I sites) and insertion of a multiple cloning site (between the *Kpn*I and *Xba*I sites) from pBluescript II (Stratagene). pTK-Bcl-2 and pTK-Bcl-x_L were created by the insertion of human Bcl-2 and Bcl-x_L cDNA sequences, respectively, into pTKPRMCS. pTK-E1B19K was constructed by the insertion of the E1B19K fragment into pTKPRMCS. As shown in Fig. 3(b), plasmids expressing E1B19K, Bcl-2 or Bcl-x_L restored vector production of the E1B19K deletion mutant to levels equivalent to that produced by the wild-type pE1 plasmid. The use of the medium strength HSV-*tk* promoter to drive the expression

of the Bcl-2 homologues was essential for helper function. CMV-driven constructs produced low vector yields in a dominant fashion and caused a substantial increase in apoptosis (data not shown).

The fact that E1B19K mutants can be complemented by similarly anti-apoptotic cellular homologues such as Bcl-2 or Bcl-x_L suggests a common mechanism, the inhibition of Bak/Bax-mediated apoptosis. Interestingly, no increase in DNA ladder formation is seen in HeLa cells when transfected with E1B19K mutant plasmids relative to wild-type plasmids (data not shown). Consequently, the mechanism of vector production augmentation is not clear.

Current transfection-based AAV vector production methods are sufficient to commercially support gene therapy applications with large doses and small patient populations (e.g. haemophilia, other genetic diseases) or applications with small doses and large patient populations (e.g. Parkinson's disease). Applications with large doses and large patient populations (e.g. heart failure) will be a challenge for transfection-based production methods that scale linearly. Consequently, the construction of a producer cell line that is both helper virus-free, and suspension culture-adaptable, is of great interest. This is a formidable task since many of the viral helper proteins are toxic to the cell either alone (e.g. E2A) or in combination with other helper functions (e.g. E4orf6 and E1B55K, E1A and *rep*). The task is further complicated by genes such as E1B19K that must be expressed in a rather precise manner. Packaging cell lines containing inducible E1 genes, along with the E2a, VA and E4 regions, and an integrated AAV vector have been produced but were found to suffer from relatively low vector yield and substantial production instability (Qiao *et al.*, 2002). Both of these problems were likely due to, or exacerbated by, helper gene toxicity. Our data indicates that one source of toxicity, the inhibition of host mRNA nuclear export mediated by the E4orf6/E1B55K heterodimer, could be eliminated by not including the E1B55K gene in packaging cell lines.

Defining the minimum set of helper genes necessary for efficient vector production is the first step in creating suitable packaging cell lines for AAV vectors. Using our transfection-based assay, we define that set to be E1A, E1B19K, the VA RNAs, E2A and E4orf6 genes.

Acknowledgements

We thank Dr Lawrence H. Boise for providing the Bcl-x_L cDNA, and Dr Michael Lochrie and Dr Matthew Weitzman for manuscript review and helpful comments. We also thank Dr Tatsuya Nomoto and Ms Miyoko Mitsu for their encouragement and support. This work was supported in part by a Grant-in-Aid for Scientific Research on Priority Areas from the Ministry of Education, Science, Sports and Culture of Japan; a grant for Research on Human Genome and Gene Therapy from the Ministry of Health, Labour and Welfare of Japan; Core Research for Evolutional Science and Technology (CREST) of the Japan Science and Technology Corporation (JST); and a Jichi Medical School young investigator award.

References

Allen, J. M., Debelak, D. J., Reynolds, T. C. & Miller, A. D. (1997). Identification and elimination of replication-competent adeno-associated virus (AAV) that can arise by nonhomologous recombination during AAV vector production. *J Virol* **71**, 6816–6822.

Allen, J. M., Halbert, C. L. & Miller, A. D. (2000). Improved adeno-associated virus vector production with transfection of a single helper adenovirus gene, E4orf6. *Mol Ther* **1**, 88–95.

Atchinson, R. W., Casto, B. C. & Hammon, W. M. (1965). Adenovirus-associated defective virus particles. *Science* **149**, 754–756.

Buller, R. M., Janik, J. E., Sebring, E. D. & Rose, J. A. (1981). Herpes simplex virus types 1 and 2 completely help adenovirus-associated virus replication. *J Virol* **40**, 241–247.

Carter, B. J., Antoni, B. A. & Klessig, D. F. (1992). Adenovirus containing a deletion of the early region 2A gene allows growth of adeno-associated virus with decreased efficiency. *Virology* **191**, 473–476.

Chang, L. S. & Shenk, T. (1990). The adenovirus DNA-binding protein stimulates the rate of transcription directed by adenovirus and adeno-associated virus promoters. *J Virol* **64**, 2103–2109.

Gao, G., Qu, G., Burnham, M. S. & 7 other authors (2000). Purification of recombinant adeno-associated virus vectors by column chromatography and its performance *in vivo*. *Hum Gene Ther* **11**, 2079–2091.

Jooss, K., Yang, Y., Fisher, K. J. & Wilson, J. M. (1998). Transduction of dendritic cells by DNA viral vectors directs the immune response to transgene products in muscle fibers. *J Virol* **72**, 4212–4223.

Liang, X. H., Mungal, S., Ayscue, A., Meissner, J. D., Wodnicki, P., Hockenbery, D., Lockett, S. & Herman, B. (1995). Bcl-2 proto-oncogene expression in cervical carcinoma cell lines containing inactive p53. *J Cell Biochem* **57**, 509–521.

Lowe, S. W., Ruley, H. E., Jacks, T. & Housman, D. E. (1993). p53-dependent apoptosis modulates the cytotoxicity of anticancer agents. *Cell* **74**, 957–967.

Matsushita, T., Elliger, S., Elliger, C., Podsakoff, G., Villarreal, L., Kurtzman, G. J., Iwaki, Y. & Colosi, P. (1998). Adeno-associated virus vectors can be efficiently produced without helper virus. *Gene Ther* **5**, 938–945.

Pilder, S., Logan, J. & Shenk, T. (1984). Deletion of the gene encoding the adenovirus 5 early region 1b 21,000-molecular-weight polypeptide leads to degradation of viral and host cell DNA. *J Virol* **52**, 664–671.

Pilder, S., Moore, M., Logan, J. & Shenk, T. (1986). The adenovirus E1B-55K transforming polypeptide modulates transport or cytoplasmic stabilization of viral and host cell mRNAs. *Mol Cell Biol* **6**, 470–476.

Qiao, C., Li, J., Skold, A., Zhang, X. & Xiao, X. (2002). Feasibility of generating adeno-associated virus packaging cell lines containing inducible adenovirus genes. *J Virol* **76**, 1904–1913.

Querido, E., Marcellus, R. C., Lai, A., Charbonneau, R., Teodoro, J. G., Ketner, G. & Branton, P. E. (1997). Regulation of p53 levels by the E1B 55-kilodalton protein and E4orf6 in adenovirus-infected cells. *J Virol* **71**, 3788–3798.

Rabinowitz, J. E. & Samulski, J. (1998). Adeno-associated virus expression systems for gene transfer. *Curr Opin Biotechnol* **9**, 470–475.

Samulski, R. J. & Shenk, T. (1988). Adenovirus E1B 55-Mr polypeptide facilitates timely cytoplasmic accumulation of adeno-associated virus mRNAs. *J Virol* **62**, 206–210.

Schlehofer, J. R., Ehrbar, M. & zur Hausen, H. (1986). Vaccinia virus, herpes simplex virus, and carcinogens induce DNA amplification in a human cell line and support replication of a helpervirus dependent parvovirus. *Virology* **152**, 110–117.

Steegenga, W. T., Riteco, N., Jochemsen, A. G., Fallaux, F. J. & Bos, J. L. (1998). The large E1B protein together with the E4orf6 protein

target p53 for active degradation in adenovirus infected cells. *Oncogene* **16**, 349–357.

Tratschin, J. D., West, M. H., Sandbank, T. & Carter, B. J. (1984). A human parvovirus, adeno-associated virus, as a eucaryotic vector: transient expression and encapsidation of the procaryotic gene for chloramphenicol acetyltransferase. *Mol Cell Biol* **4**, 2072–2081.

Walz, C., Deprez, A., Dupressoir, T., Durst, M., Rabreau, M. & Schlehofer, J. R. (1997). Interaction of human papillomavirus type 16 and adeno-associated virus type 2 co-infecting human cervical epithelium. *J Gen Virol* **78**, 1441–1452.

Ward, P., Dean, F. B., O'Donnell, M. E. & Berns, K. I. (1998). Role of the adenovirus DNA-binding protein in *in vitro* adeno-associated virus DNA replication. *J Virol* **72**, 420–427.

West, M. H., Trempe, J. P., Tratschin, J. D. & Carter, B. J. (1987). Gene expression in adeno-associated virus vectors: the effects of chimeric mRNA structure, helper virus, and adenovirus VA1 RNA. *Virology* **160**, 38–47.

Xiao, X., Li, J. & Samulski, R. J. (1998). Production of high-titer recombinant adeno-associated virus vectors in the absence of helper adenovirus. *J Virol* **72**, 2224–2232.

Gene Therapy (2005) 12, 203–210

www.nature.com/gt

RESEARCH ARTICLE

Efficient and stable Sendai virus-mediated gene transfer into primate embryonic stem cells with pluripotency preserved

K Sasaki[1,2], M Inoue[3], H Shibata[1], Y Ueda[3], S-i Muramatsu[4], T Okada[1], M Hasegawa[3], K Ozawa[1] and Y Hanazono[1]

[1]*Center for Molecular Medicine, Jichi Medical School, Minamikawachi, Tochigi, Japan;* [2]*Department of Plastic and Reconstructive Surgery, Faculty of Medicine, University of Tokyo, Bunkyo-ku, Tokyo, Japan;* [3]*DNAVEC Corporation, Tsukuba, Ibaraki, Japan; and* [4]*Department of Neurology, Jichi Medical School, Minamikawachi, Tochigi, Japan*

Efficient gene transfer and regulated transgene expression in primate embryonic stem (ES) cells are highly desirable for future applications of the cells. In the present study, we have examined using the nonintegrating Sendai virus (SeV) vector to introduce the green fluorescent protein (GFP) gene into non-human primate cynomolgus ES cells. The GFP gene was vigorously and stably expressed in the cynomolgus ES cells for a year. The cells were able to form fluorescent teratomas when transplanted into immunodeficient mice. They were also able to differentiate into fluorescent embryoid bodies, neurons, and mature blood cells. In addition, the GFP expression levels were reduced dose-dependently by the addition of an anti-RNA virus drug, ribavirin, to the culture. Thus, SeV vector will be a useful tool for efficient gene transfer into primate ES cells and the method of using antiviral drugs should allow further investigation for regulated SeV-mediated gene expression.
Gene Therapy (2005) **12**, 203–210. doi:10.1038/sj.gt.3302409
Published online 14 October 2004

Keywords: *primate embryonic stem cell; Sendai virus vector; gene transfer; green fluorescent protein; pluripotency; ribavirin*

Introduction

Since human embryonic stem (ES) cell lines have the ability to both proliferate indefinitely and differentiate into multiple tissue cells,[1,2] they are expected to have clinical applications as well as to serve as models for basic research and drug development. Although efficient and stable gene transfer into primate ES cells would be useful for such purposes, it has been difficult and only lentiviral vectors have been successful in achieving it.[3–5] We have previously developed Sendai virus (SeV) vectors that replicate in the form of negative-sense single-stranded RNA in the cytoplasm of infected cells and do not go through a DNA phase.[6] SeV vectors can efficiently introduce foreign genes without toxicity into airway epithelial cells,[7] vascular tissue,[8] skeletal muscle,[9] synovial cells,[10] retinal tissue,[11] and hematopoietic progenitor cells.[12] Here we report that the SeV-mediated gene transfer into primate ES cells is very efficient and stable even after the terminal differentiation of the cells. In addition, we show that SeV-mediated transgene expression levels can be reduced by the addition of a ribonucleoside analog, ribavirin, to the culture. Ribavirin is a mutagen and inhibitor of viral RNA polymerase.[13,14] It shows antiviral activity against a variety of RNA viruses and is used to treat infections of hepatitis C virus in combination with interferon-α[15,16] and of lassa fever virus.[17] The method of using antiviral drugs might offer a novel approach for regulated SeV-mediated gene expression in primate ES cells.

Correspondence: Dr Y Hanazono, Center for Molecular Medicine, Jichi Medical School, 3311-1 Yakushiji, Minamikawachi, Tochigi 329-0498, Japan
Received 20 April 2004; accepted 27 August 2004; published online 14 October 2004

Results

SeV-mediated gene transfer into ES cells

In this study, we have used an SeV vector, which is capable of self-replication but incapable of transmitting to other cells.[6] The vector does not encode the fusion (F) protein (Figure 1a), which is essential for viral entry into cells. It can be propagated only in a packaging cell line expressing the F protein. The green fluorescent protein (GFP) gene was introduced after the leader sequence of the vector genome. Cynomolgus ES cells[18] were exposed to the SeV vector for 24 h. Flow cytometric analysis at 2 days after infection showed that 15, 38, and 61% of cells fluoresced at 2, 10, and 50 transducing units (TU) per cell, respectively (Figure 1b). The gene transfer efficiency of about 60% is comparable to or even better than that for lentiviral vectors.[3] We confirmed that the undifferentiated cell fractions remained unchanged after the infection with SeV vector, as assessed by the expression of undifferentiated markers, alkaline phosphatase and SSEA-4 (data not shown). The GFP expression after infection was stable at least for a month. On the other hand, the GFP gene transfer to cynomolgus ES cells with adenovirus- and adeno-associated virus (AAV)-based vectors resulted in much lower expression levels (<20% by flow cytometry) and the levels declined to zero within a week after infection (Figure 1c).

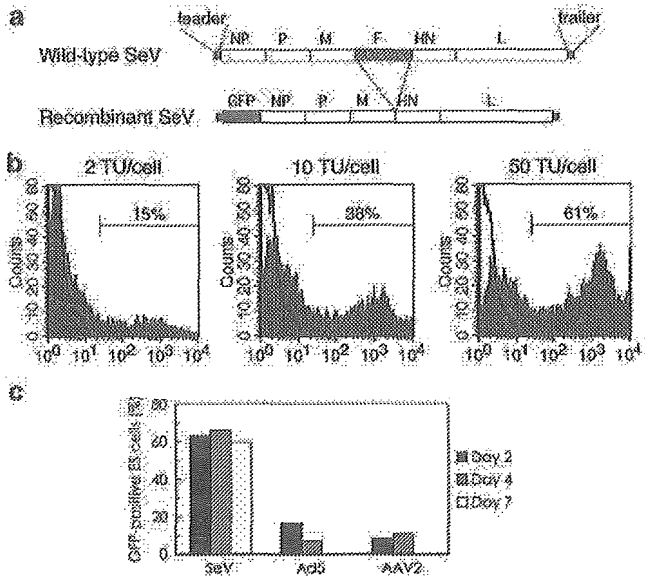

Figure 1 High-level transgene expression in cynomolgus ES cells after infection with SeV vector. (a) Schematic diagrams of the wild-type SeV genome and recombinant F-defective SeV carrying the GFP gene (SeV vector in this study). The SeV genome is 15 384 nucleotides long and its genes (NP, P, M, F, HN, and L) are in order from 3′ to 5′ in the negative-strand RNA. In the SeV vector, the entire fusion (F) gene was removed and the GFP gene was introduced at a unique NotI site between the leader sequence and NP gene. (b) The GFP expression by the SeV vector in cynomolgus ES cells. Cynomolgus ES cells were infected with the SeV vector at 2, 10, and 50 TU/cell. The flow cytometric profiles at day-2 postinfection are shown in gray. The white areas indicate uninfected ES cells. The fractions of GFP-positive cells are indicated. (c) The GFP expression levels in cynomolgus ES cells infected with the SeV (50 TU/cell), adenovirus serotype 5 (Ad5, 3.4×10^2 g.c./cell), and AAV serotype 2 (AAV2, 2.4×10^4 g.c./cell) vectors. The fractions of GFP-positive cells were examined by flow cytometry at 2, 4, and 7 days postinfection.

We plucked fluorescent ES cell colonies under a fluorescent microscope once at 1 month after infection and propagated them. After this selection procedure, approximately 90% of the ES cells expressed GFP (Figure 2a and b) and the high-level expression was stable for a year as assessed by flow cytometry (Figure 2c, upper). The mean fluorescence intensity per cell was also stable (Figure 2c, lower), indicating that the replicating vector genome was almost equally delivered to each cell of all progeny. The self-replication of the SeV vector in infected cells was confirmed by RNA-PCR that amplified the viral RNA genomic sequence (Figure 3a). The GFP cDNA sequence, however, could not be detected by DNA-PCR in the infected cells (Figure 3b), indicating that no DNA phase was involved in the GFP expression.

Pluripotency of infected ES cells

The SeV-infected, fluorescent cynomolgus ES cells were able to form fluorescent tumors when transplanted into immunodeficient mice (Figure 4a–c). The fluorescence was observed uniformly by fluorescent microcopy (Figure 4d and e). The tumors consisted of all three embryonic germ layer cells (Figure 4f–i). Thus, the SeV-infected ES cells were capable of forming teratomas and the SeV infection did not spoil the pluripotency of ES cells. The infected, fluorescent cynomolgus ES cells were also able to generate fluorescent embryoid bodies (Figure 5a and b), MAP-2-positive neurons (Figure 5c), clonogenic hematopoietic colonies (Figure 5d and e), and mature functional (NBT test-positive) neutrophils (Figure 5f and g), all of which fluoresced. In addition, the GFP expression levels were not decreased during the teratoma formation or differentiation, indicating that no 'silencing' of the transgene occurred.

Drug-inducible reduction of transgene expression

Next, we examined whether ribavirin inhibits the replication and transcription of the SeV vector resulting in a reduction of transgene expression. We first used a rhesus monkey kidney cell line (LLC-MK2) to test the effect of ribavirin on the replication and transcription of the SeV vector. LLC-MK2 is a standard control cell line for SeV infection. Ribavirin was added at various concentrations 2 days after the infection. The formation of viral particles quantified by the hemagglutination assay decreased drastically upon the addition of ribavirin (Figure 6a). The decrease was dependent on the dose of ribavirin. The GFP expression was also depressed dose-dependently (Figure 6b). Thus, ribavirin dose-dependently inhibits the replication and transcription of the SeV vector in LLC-MK2 cells. The toxicity associated with ribavirin was not observed in LLC-MK2 cells.

We then examined the effect of ribavirin on SeV-infected, fluorescent cynomolgus ES cells. The addition of ribavirin also resulted in a dose-dependent reduction of GFP expression in the cells (Figure 6c). Although the GFP expression was almost completely inhibited after a 3-day exposure with 4 mM of ribavirin, the cells could not be propagated thereafter. Ribavirin at high concentrations (>1 mM) hampered the proliferation of cynomolgus ES cells. With lower concentrations (0.5–0.75 mM) of ribavirin, the GFP expression level decreased by half. After the discontinuation of ribavirin treatment, the cells could be propagated and nearly regained the original level of GFP expression. The undifferentiated cell fractions were unchanged after the discontinuation as assessed by alkaline phosphatase and SSEA-4 staining (Figure 6d).

Discussion

There are several advantages in using SeV vectors over other vectors. (i) SeV vectors can infect nondividing, quiescent cells as well as dividing cells unlike oncoretroviral vectors.[7–11] Thus, they can be used to infect cells that are terminally differentiated as well as at various stages of differentiation, whether they are dividing or not. (ii) SeV vector-mediated gene transfer does not require a DNA phase. Thus, there is no concern about the unwanted integration of foreign sequences into the host genome unlike with oncoretroviral or lentiviral vectors. (iii) Transgene expression is stable even in dividing cells since the SeV vector replicates by itself in the cytoplasm of host cells. On the other hand, gene transfer using nonreplicating adenoviral and AAV vectors resulted in decreased levels of transgene expression in dividing cells over time, since the non-replicating transgene was

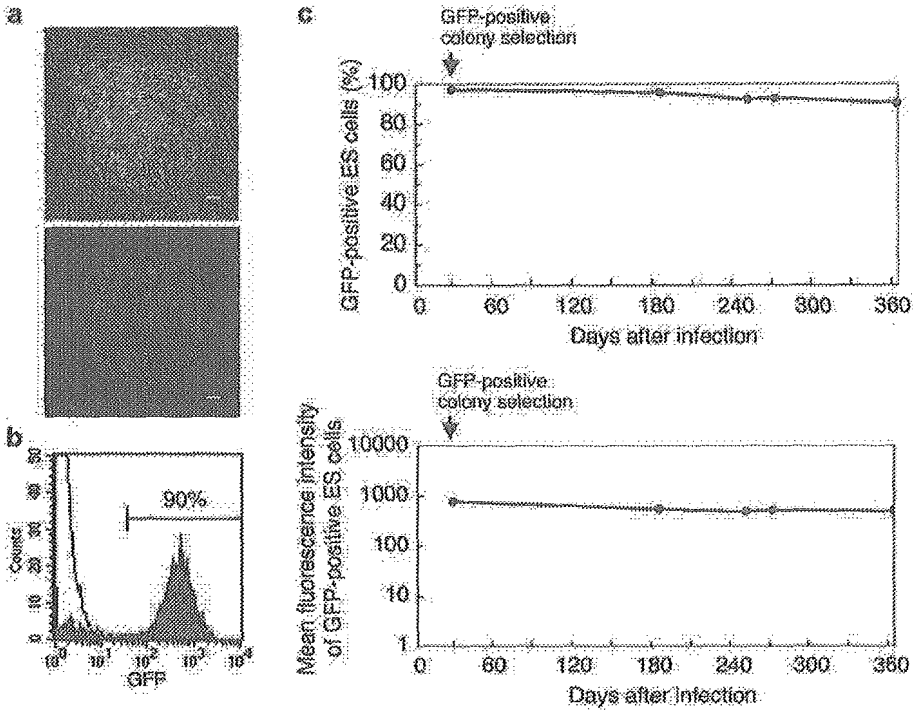

Figure 2 Stable SeV-mediated transgene expression in cynomolgus ES cells. Fluorescent ES cell colonies were plucked under a fluorescent microscope once at 1 month after infection and the cells were further propagated. (a) Phase-contrast (upper) and fluorescence (lower) images of a cynomolgus ES cell colony at day 370 after infection. Bar = 100 μm. (b) Flow cytometric analysis of SeV-infected cynomolgus ES cells at day 370 after infection (shown in green). The percentage of GFP-positive cells is indicated. Uninfected, parental cynomolgus ES cells are indicated by another line (white area). (c) The percentage of GFP-positive cells (upper) and mean fluorescence intensity per GFP-positive cell (lower) after infection with the SeV vector at 10 TU/cell are shown as a function of time (days).

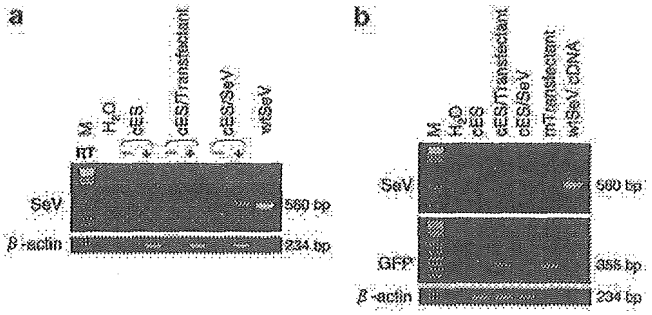

Figure 3 DNA-independent replication and transcription of SeV vector. Total cellular RNA and DNA were extracted from cynomolgus ES cells at day 284 after infection with the SeV vector. RNA-PCR (a) and DNA-PCR (b) for the SeV RNA genome or GFP sequence were conducted. The cynomolgus β-actin sequence was used as an internal control. In the RNA-PCR (a), negative results obtained without reverse transcriptase (designated RT−) confirmed that the amplified products were not derived from cellular DNA. M, 100-kb DNA ladder; cES, naive cynomolgus ES cells; cES/Transfectant, cynomolgus ES cells stably expressing the GFP gene after transfection,[33] cES/SeV, cynomolgus ES cells infected with the SeV vector; wtSeV, wild-type SeV genome; mTransfectant, a GFP-positive mouse cell line after transfection.

diluted out. (iv) The SeV vector is much less unlikely to generate wild-type virus *in vitro* or *in vivo* than oncoretroviral and lentiviral vectors, since homologous recombination between RNA genomes is very rare indeed in negative-strand RNA viruses.[19] (v) The SeV genome is not subject to cellular epigenetic modifications such as methylation, and thus it is unlikely that methylation-based silencing of transgene expression occurs.

No cytotoxic or differentiating effect on ES cells associated with the SeV infection was observed in our study. However, the wild-type SeV contains immunogenic surface proteins, hemagglutinin-neuraminidase (HN) and F proteins, which potentially induce antibody responses.[20,21] For future clinical applications, it would be desired that as many viral genes as possible are deleted from the vector backbone to permit reapplication, improve the safety, and lessen the possible toxicity of SeV vectors. To this end, we have developed a series of attenuated SeV vectors that are F gene-deleted,[6] F gene-deleted with preferable mutations,[22] M gene-deleted,[23] or have deletions of both F and M genes.[24] The modified vectors would be safer for *in vivo* use.

Ribavirin at high concentrations seems toxic to ES cells; presumably, it directly hampers viability and proliferation potential of ES cells. However, we cannot tell whether the observed toxicity is simply due to its toxicity to ES cells, as feeder cells are more highly sensitive to ribavirin than ES cells. In fact, while feeder cells died at 1 mM of ribavirin, cocultured ES cells were alive at this concentration for some time. Cynomolgus ES cells lose pluripotency and proliferation potential without feeder cells. Thus, the observed toxicity to ES cells may also be a secondary event following the injury of feeder cells. Whether the cytotoxicity is primary or secondary, it will be necessary to find modified compounds of less cytotoxicity.

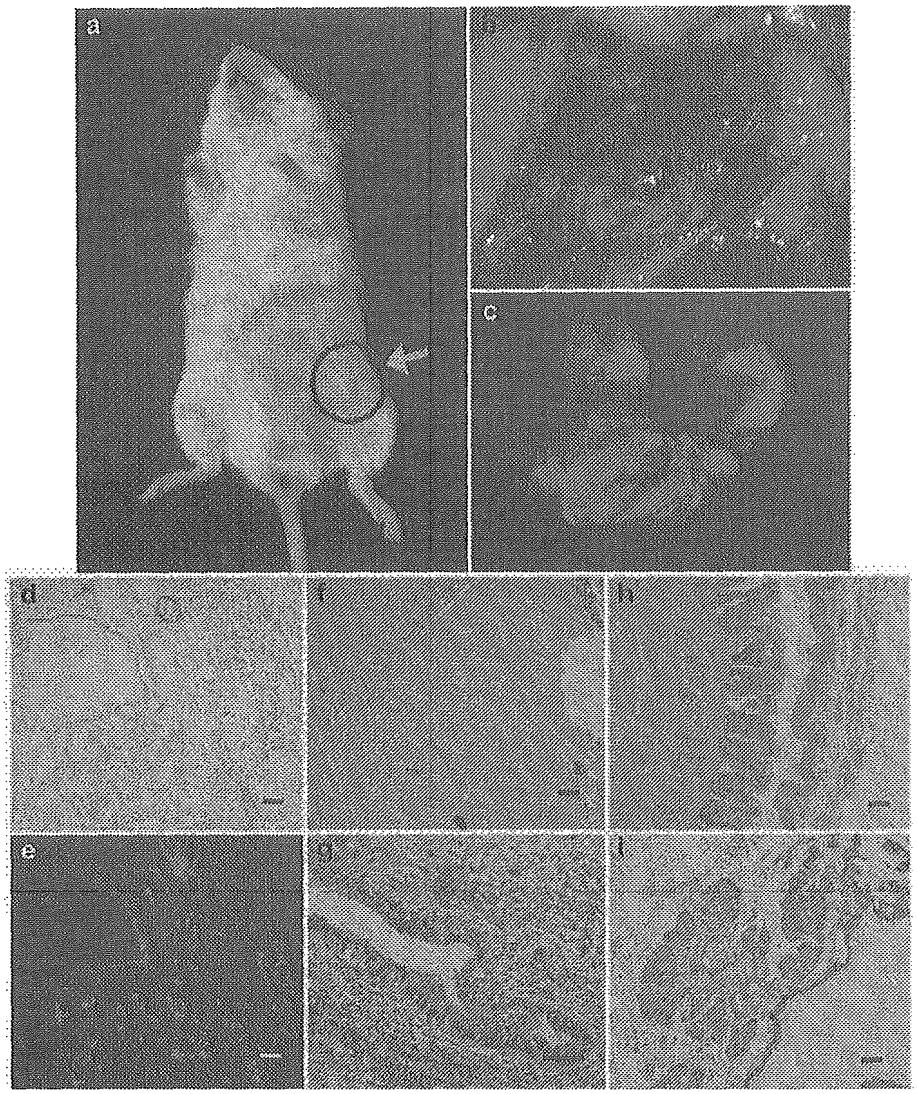

Figure 4 Pluripotency of SeV-infected cynomlgus ES cells. Tumors formed in NOD-SCID mice after inoculation of the SeV-infected cynomolgus ES cells (a). The tumor was fluorescing ((b), bright field; (c), dark field). Fluorescence was observed uniformly in the tumor under a fluorescent microscope ((d), bright field; (e), dark field). The tumor contained all three embryonic germ layer cells; cartilage (f), ciliated columnar epithelium (g), skin (h), and sebaceous gland (i) (stained with hematoxylin and eosin). Bar = 100 μm.

Materials and methods

Cell culture

Cynomolgus ES cells (CMK6) were maintained on a feeder layer of mitomycin C (Kyowa, Tokyo, Japan)-treated mouse (BALB/c) embryonic fibroblasts as described previously.[18] The culture medium consisted of Dulbecco's modified Eagle's medium (DMEM)/F12 (Invitrogen, Carlsbad, CA, USA) supplemented with 15% ES cell-qualified fetal calf serum (FCS; Invitrogen), 0.1 mM 2-mercaptoethanol (Sigma, St Louis, MO, USA), 2 mM glutamine (Invitrogen), 0.1 mM nonessential amino acids (Invitrogen), and antibiotics (100 U/ml penicillin and 100 μg/ml streptomycin, Irvine Scientific, Santa Ana, CA, USA). The ES cell colonies were routinely passaged every 3–4 days after dissociation with a combined approach of 0.25% trypsin (Invitrogen) digestion and mechanical cutting. Alkaline phosphatase staining was conducted with an Alkaline Phosphatase Chromogen Kit (Biomeda, Foster City, CA, USA). Embryoid bodies were produced by culturing ES cell aggregates in Petri dishes. LLC-MK2 cells (1×10^6) were grown in six-well plates and cultured in Eagle's minimal essential medium (Invitrogen) supplemented with 10% FCS.

Vectors

The F-defective SeV vector carrying the GFP gene was constructed as previously described.[6] The vector titer was 1.8×10^9 TU/ml determined by counting fluorescent cells after the infection of LLC-MK2 cells. Gene transfer was conducted by adding various concentrations of the SeV vector solution to culture media. After 24 h of incubation, the cells were washed twice with phosphate-buffered saline (PBS) and fresh medium was added. In some experiments, ribavirin (1-β-D-ribofuranosyl-1,2,4-triazole-3-carboxamide; Sigma) was added at various concentrations to the culture media after infection. The

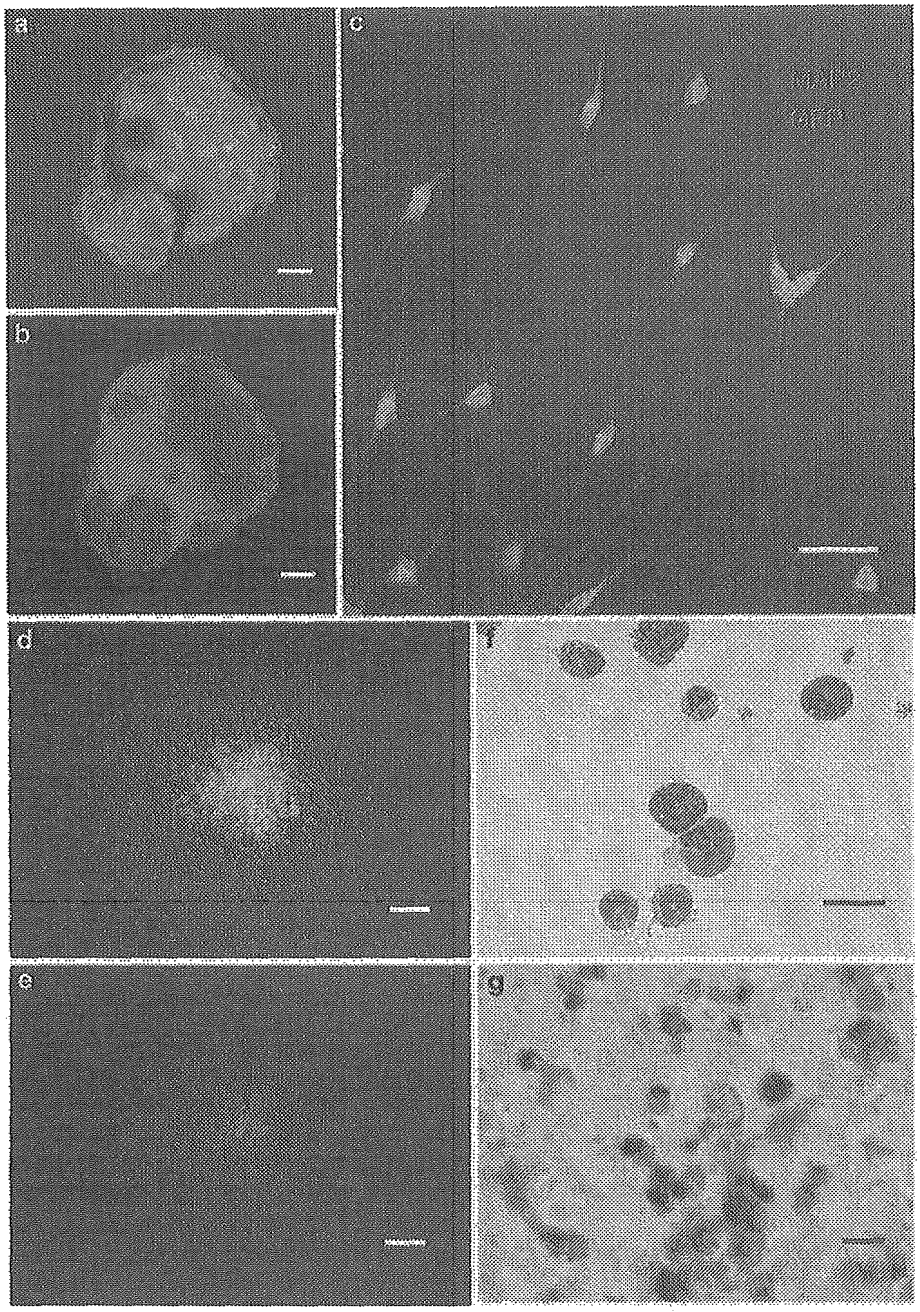

Figure 5 Stable transgene expression during differentiation. A day-20 cystic embryoid body was observed under a fluorescent phase-contrast microscope, confirming that the embryoid body was fluorescing ((a), bright field; (b), dark field). After infection with the SeV vector, fluorescent cynomolgus ES cells differentiated into neural cells. Double immunostaining with anti-GFP (green) and ant-MAP-2 (red) confirmed that differentiated neural cells expressed GFP (c). Yellow cells indicate GFP-expressing neurons. SeV-infected, fluorescent cynomolgus ES cells also differentiated into fluorescent hematopoietic cells. A clonogenic hematopoietic colony was fluorescing ((d) bright field; (e), dark field). A cytospin specimen of hematopoietic colony cells (Wright–Giemsa staining) showed that the cells were mature granulocytes (f). The infected ES cell-derived, fluorescent neutrophils were positive for NBT (stained in black (g)). Bar = 100 μm (a, b, g); 50 μm (c, f); 500 μm (d, e).

viral particles in infected cells were quantified by a hemagglutination assay as described previously.[25]

An adenovirus serotype 5-based vector carrying the GFP gene was constructed as reported.[26] It contained the cytomegalovirus (CMV) promoter, simian virus (SV)-40 intron, and SV-40 polyadenylation signal. An AAV serotype 2-based vector expressing the GFP gene under the control of the chicken β-actin promoter with the CMV immediate-early enhancer (a gift from Dr J Miyazaki) was prepared as described previously.[27] Gene transfer experiments were performed using 3.4×10^2 genome copies (g.c.)/cell of the adenoviral vector or 2.4×10^4 g.c./cell of the AAV vector. The period of exposure was 48 h.

Flow cytometry

GFP and SSEA-4 expression was analyzed on a FACScan (Becton Dickinson, Franklin Lakes, NJ, USA) using the

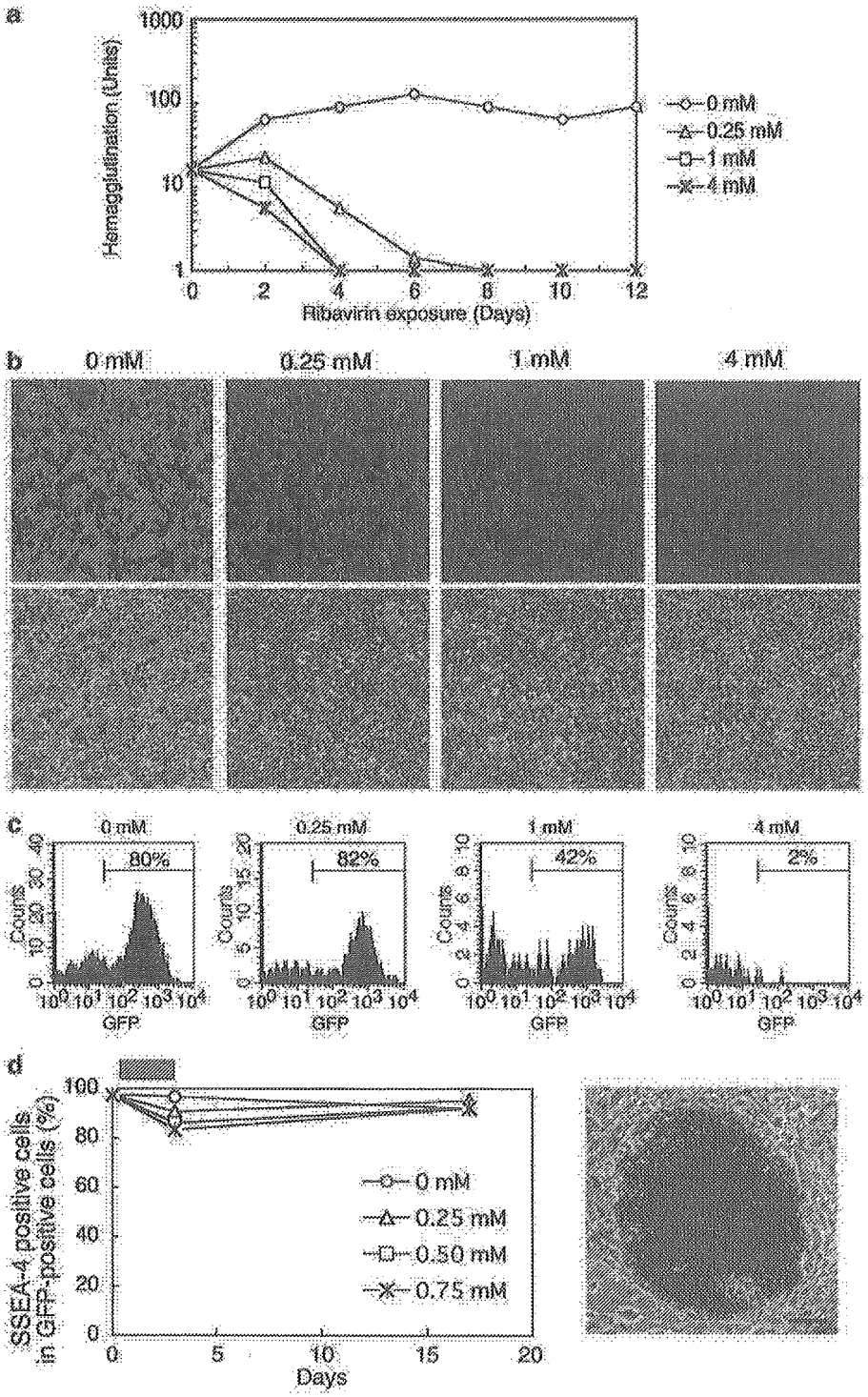

Figure 6 *Ribavirin-regulated transgene expression. (a) A rhesus kidney cell line (LLC-MK2) was infected with the SeV vector at 3 TU/cell. Ribavirin was started at various concentrations on day 2 after the infection. The formation of viral particles in the infected LLC-MK2 cells was examined by the hemagglutination assay. (b) The ribavirin-treated LLC-MK2 cells were observed under a fluorescent microscope after an 8-day exposure of ribavirin (upper, dark field; lower, bright field). (c) Ribavirin was added at various concentrations to the SeV-infected, fluorescent cynomolgus ES cells. The GFP expression was assessed by flow cytometry after a 3-day exposure of ribavirin. (d) The fractions of SSEA-4-positive ES cells were assessed by flow cytometry with anti-SSEA-4 before and after a 3-day exposure of ribavirin and are shown as a function of time (days) in the left panel. A gray bar indicates ribavirin treatment. ES cells were stained for alkaline phosphatase (in red) at day 21 after a 3-day exposure of 0.75 mM ribavirin and are shown in the right panel. Bar = 100 μm.*

CellQuest software (Becton Dickinson). For SSEA-4 staining, cells were incubated with a primary antibody, anti-SSEA-4 (MC-813-70; Chemicon, Temecula, CA, USA), and then a secondary antibody, PE-conjugated F(ab')2 fragment of rabbit anti-mouse immunoglobulins (DakoCytomation, Glostrup, Denmark). Cocultured BALB/c feeder cells could be distinguished from cynomolgus ES cells by using PE-conjugated anti-mouse

H-2d (SF1-1.1; PharMingen, San Diego, CA, USA), which does not react to cynomolgus cells but does react to BALB/c cells.

Teratoma formation

Cynomolgus ES cells (approximately 10^6 cells per site) were injected subcutaneously into the hind leg of 6- to 8-week-old nonobese diabetic/severe combined immunodeficient mice (Jackson Laboratory, Bar Harbor, ME, USA). The resulting tumors (usually 9–12 weeks after the injection) were dissected and fixed in 4% paraformaldehyde. For histological analysis, samples from the tumors were embedded in paraffin and stained with hematoxylin and eosin. To observe GFP fluorescence, samples were embedded in OTC compound (Sakura, Zoeterwoude, Netherlands), frozen, sectioned, and examined under a fluorescence microscope.

Hematopoietic differentiation

The mouse bone marrow stromal cell line OP9 was maintained in α-modified minimum essential medium (Invitrogen) supplemented with 20% FCS as described previously.[28] For induction of hematopoietic differentiation, ES cells were seeded onto a mitomycin C-treated confluent OP9 cell layer in six-well plates. Medium to support the differentiation was described elsewhere.[29] Cells at day 18 were placed in Methocult GF+ media (StemCell Technologies, Vancouver, Canada) at 1×10^4 and 1×10^5 cells per plate and clonogenic hematopoietic colonies were produced. After 14 days, individual colonies were removed and spun onto glass slides. Cells were stained with the Wright–Giemsa method. The nitro blue tetrazolium (NBT, Sigma) reduction test was performed on the cells as a granulocyte functional assay according to a previously described method.[30]

Neural differentiation

The induction of neural differentiation was carried out as described previously.[31] Day-4 embryoid bodies were plated onto tissue culture dishes and nestin-positive cells were selected in DMEM/F12 medium supplemented with 5 μg/ml of insulin (Sigma), 50 μg/ml of transferrin (Sigma), 30 nM selenium chloride (Sigma), and 5 μg/ml of fibronectin (Sigma) for 5 days. Cells were then trypsinized and plated in polyornithine-coated dishes (15 μg/ml) and expanded in N2 medium[32] supplemented with 1 μg/ml of laminin (Sigma) and 10 μg/ml of basic fibroblast growth factor (bFGF; Roche, Basel, Switzerland) for 6 days. Differentiation was induced by removal of bFGF. To confirm the neural differentiation, cells were stained with anti-human MAP-2. Briefly, cells were fixed in 4% paraformaldehyde in PBS and incubated with anti-human MAP-2 (HM-2; Sigma; diluted 1:4000) and then by Alexa Fluor 594-labeled antibody (diluted 1:500; Molecular Probe, Eugene, OR, USA). The samples were examined under a fluorescence microscope.

DNA-PCR

DNA-PCR for the SeV genome and GFP sequences was carried out as follows. DNA was extracted using the QIAamp DNA mini kits (Qiagen, Hilden, Germany) and 250 ng was used for each PCR with ExTaq (Takara, Shiga, Japan). Amplification conditions were 30 cycles of 94°C for 1 min, a variable annealing temperature (noted below) for 1 min, and 72°C for 1 min. The amplified products were run on 2% agarose gel and visualized by ethidium bromide staining. Primer sequences, annealing temperatures and product sizes were as follows: the SeV vector genome sequence: 5′-AGA GAA CAA GAC TAA GGC TAC C-3′ and 5′-ACC TTG ACA ATC CTG ATG TGG-3′ (55°C, 580 bp); the GFP sequence: 5′-CGT CCA GGA GCG CAC CAT CTT C-3′ and 5′-GGT CTT TGC TCA GGG CGG ACT-3′ (60°C, 356 bp). the cynomolgus β-actin sequence: 5′-CAT TGT CAT GGA CTC TGG CGA CGG-3′ and 5′-CAT CTC CTG CTC GAA GTC TAG GGC-3′ (60°C, 234 bp).

RNA-PCR

RNA-PCR for the SeV RNA genomic sequence was carried out as follows. Total RNA was extracted using RNA STAT-60 (Tel-Test, Friendswood, TX, USA). Reverse transcription was conducted by using Taqman reverse transcription reagents (Applied Biosystems, Foster City, CA, USA). The product (250 ng) after the reverse transcription was used for the subsequent PCR as described above.

Acknowledgements

Cynomolgus ES cells were provided by Norio Nakatsuji (Kyoto University, Kyoto, Japan), Yasushi Kondo (Tanabe Seiyaku Co. Ltd, Osaka, Japan), and Ryuzo Torii (Shiga University of Medical Science, Shiga, Japan). OP9 cells were provided by Toru Nakano (Osaka University, Osaka, Japan). We thank Yujiro Tanaka and Takayuki Asano for cultivating cynomolgus ES cells and Takeshi Hara for conducting NBT tests. We also thank Natsuko Kurosawa for technical assistance.

References

1 Thomson JA *et al.* Embryonic stem cell lines derived from human blastocysts. *Science* 1998; **282**: 1145–1147.
2 Reubinoff BE *et al.* Embryonic stem cell lines from human blastocysts: somatic differentiation *in vitro*. *Nat Biotechnol* 2000; **18**: 399–404.
3 Asano T *et al.* Highly Efficient gene transfer into primate embryonic stem cells with a simian lentivirus vector. *Mol Ther* 2002; **6**: 162–168.
4 Ma Y *et al.* High-level sustained transgene expression in human embryonic stem cells using lentiviral vectors. *Stem Cells* 2003; **21**: 111–117.
5 Gropp M *et al.* Stable genetic modification of human embryonic stem cells by lentiviral vectors. *Mol Ther* 2003; **7**: 281–287.
6 Li HO *et al.* A cytoplasmic RNA vector derived from nontransmissible Sendai virus with efficient gene transfer and expression. *J Virol* 2000; **74**: 6564–6569.
7 Yonemitsu Y *et al.* Efficient gene transfer to airway epithelium using recombinant Sendai virus. *Nat Biotechnol* 2000; **18**: 970–973.
8 Masaki I *et al.* Recombinant Sendai virus-mediated gene transfer to vasculature: a new class of efficient gene transfer vector to the vascular system. *FASEB J* 2001; **15**: 1294–1296.
9 Shiotani A *et al.* Skeletal muscle regeneration after insulin-like growth factor I gene transfer by recombinant Sendai virus vector. *Gene Therapy* 2001; **8**: 1043–1050.
10 Yamashita A *et al.* Fibroblast growth factor-2 determines severity of joint disease in adjuvant-induced arthritis in rats. *J Immunol* 2002; **168**: 450–457.

11 Ikeda Y *et al.* Recombinant Sendai virus-mediated gene transfer into adult rat retinal tissue: efficient gene transfer by brief exposure. *Exp Eye Res* 2002; **75**: 39–48.
12 Jin CH *et al.* Recombinant Sendai virus provides a highly efficient gene transfer into human cord blood-derived hematopoietic stem cells. *Gene Therapy* 2003; **10**: 272–277.
13 Crotty S *et al.* The broad-spectrum antiviral ribonucleoside ribavirin is an RNA virus mutagen. *Nat Med* 2000; **6**: 1375–1379.
14 Vo NV, Young KC, Lai MM. Mutagenic and inhibitory effects of ribavirin on hepatitis C virus RNA polymerase. *Biochemistry* 2003; **42**: 10462–10471.
15 McHutchison JG *et al.* Interferon alfa-2b alone or in combination with ribavirin as initial treatment for chronic hepatitis C. Hepatitis Interventional Therapy Group. *N Engl J Med* 1998; **339**: 1485–1492.
16 Davis GL *et al.* Interferon alfa-2b alone or in combination with ribavirin for the treatment of relapse of chronic hepatitis C. International Hepatitis Interventional Therapy Group. *N Engl J Med* 1998; **339**: 1493–1499.
17 McCormick JB *et al.* Lassa fever. Effective therapy with ribavirin. *N Engl J Med* 1986; **314**: 20–26.
18 Suemori H *et al.* Establishment of embryonic stem cell lines from cynomolgus monkey blastocysts produced by IVF or ICSI. *Dev Dyn* 2001; **222**: 273–279.
19 Spann KM, Collins PL, Teng MN. Genetic recombination during coinfection of two mutants of human respiratory syncytial virus. *J Virol* 2003; **77**: 11201–11211.
20 Tozawa H *et al.* Neutralizing activity of the antibodies against two kinds of envelope glycoproteins of Sendai virus. *Arch Virol* 1986; **91**: 145–161.
21 Tashiro M, Tobita K, Seto JT, Rott R. Comparison of protective effects of serum antibody on respiratory and systemic infection of Sendai virus in mice. *Arch Virol* 1989; **107**: 85–96.
22 Inoue M *et al.* Nontransmissible virus-like particle formation by F-deficient Sendai virus is temperature sensitive and reduced by mutations in M and HN proteins. *J Virol* 2003; **77**: 3238–3246.
23 Inoue M *et al.* A new Sendai virus vector deficient in the matrix gene does not form virus particles and shows extensive cell-to-cell spreading. *J Virol* 2003; **77**: 6419–6429.
24 Inoue M *et al.* Recombinant Sendai virus vectors deleted in both the matrix and the fusion genes: efficient gene transfer with preferable properties. *J Gene Med*, published online 5 May 2004. doi:10.1002/jgm.597.
25 Kato A *et al.* Initiation of Sendai virus multiplication from transfected cDNA or RNA with negative or positive sense. *Genes Cells* 1996; **1**: 569–579.
26 Okada T *et al.* Efficient directional cloning of recombinant adenovirus vectors using DNA–protein complex. *Nucleic Acids Res* 1998; **26**: 1947–1950.
27 Okada T *et al.* Adeno-associated viral vector-mediated gene therapy of ischemia-induced neuronal death. *Methods Enzymol* 2002; **346**: 378–393.
28 Nakano T, Kodama H, Honjo T. Generation of lympho-hematopoietic cells from embryonic stem cells in culture. *Science* 1994; **265**: 1098–1101.
29 Li F *et al.* Bone morphogenetic protein 4 induces efficient hematopoietic differentiation of rhesus monkey embryonic stem cells *in vitro*. *Blood* 2001; **98**: 335–342.
30 Sekhsaria S *et al.* Peripheral blood progenitors as a target for genetic correction of $p47^{phox}$-deficient chronic granulomatous disease. *Proc Natl Acad Sci USA* 1993; **90**: 7446–7450.
31 Lee SH *et al.* Efficient generation of midbrain and hindbrain neurons from mouse embryonic stem cells. *Nat Biotechnol* 2000; **18**: 675–679.
32 Johe KK *et al.* Single factors direct the differentiation of stem cells from the fetal and adult central nervous system. *Genes Dev* 1996; **10**: 3129–3140.
33 Takada T *et al.* Monkey embryonic stem cell lines expressing green fluorescent protein. *Cell Transplant* 2002; **11**: 631–635.

Journal of Thrombosis and Haemostasis, 3: 909–914

REVIEW ARTICLE

Molecular mechanisms of age-related regulation of genes

K. KURACHI and S. KURACHI

Age Dimension Research Center, National Institute of Advanced Industrial Science and Technology, Tsukuba, Ibaraki, Japan

To cite this article: Kurachi K, Kurachi S. Molecular mechanisms of age-related regulation of genes. *J Thromb Haemost* 2005; 3: 909–14.

Introduction

Age is a critical risk factor for many diseases such as thrombosis, cardiovascular diseases, cerebral vascular diseases, diabetes, cancer and Alzheimer's disease [1–10]. Although its importance has been shown clearly by many epidemiological studies, literally nothing is known about its molecular mechanisms of action.

Physiological systems are controlled by homeostatic mechanisms, maintaining them within small tolerable fluctuation ranges. Various internal or external insults, stresses or pathological conditions affect the homeostatic conditions. Importantly, homeostatic conditions of physiological systems are not constant with age, but continue changing slowly with age [11–13]. Such physiological changes may play a critical role either additively or synergistically in the initiation and development of many age-dependent diseases.

To explore the little-understood molecular mechanisms of age-dimension homeostasis, we first focused our study on the blood coagulation system, our model physiological system for the study (Fig. 1). This led to the first discovery of the molecular mechanisms of age-related gene regulation and therefore of homeostatic regulation of physiological systems. In this article, we review recent advances in this newly emerging research field.

Blood coagulation system and age

The complex formation of factor VII with tissue factor, which becomes available upon tissue injury, initiates blood coagulation [14] (Fig. 1). This initial reaction triggers cascades of reactions involving nearly 20 pro- and anticoagulant factors, resulting in a sufficient amount of stable fibrin clot production in a matter of minutes. Most cascade steps of this system are of proteolytic reactions in combination with increasing levels of plasma concentration of procoagulant factors as they go downstream, thus making blood coagulation an extremely efficient amplification system. In healthy individuals, blood coagulation activity makes a rapid increase during the perinatal stage and reaches a level similar to that of young adults at around weaning, followed by a gradual and continuous increase with age [15–19]. As demonstrated by epidemiological evidence [11,17,18,20], this appears to be due to an age-dependent increase in an imbalance between procoagulant activity and anticoagulant activities. Plasma concentration and/or activity of most known procoagulant factors (shown with arrows in Fig. 1) increase with age, whereas anticoagulant factors such as antithrombin (ATIII), TFPI and protein C, and profibrinolytic factors including plasminogen and tPA do not increase with age or, in some cases, even decrease slightly with age [20–22]. Importantly, PAI-1, an inhibitor of tPA which catalyzes plasminogen activation to plasmin, also increases its plasma concentration with age [22], thus resulting in an enhancement of procoagulant tendency. Together, this evidence indicates that as age proceeds, the balance between the overall procoagulant activity including the antifibrinolytic activity and that of the anticoagulant activity combined with the fibrinolytic activity tips toward the procoagulant state. In combination with various environmental conditions, including diet consumed, such an imbalance may contribute to an increased thrombotic tendency, particularly in elderly people [16–21,23,24].

Circulatory levels of human factor IX (hFIX), a key coagulation factor, significantly increase with advancing age in normal human populations [11,16,25]. In contrast, circulatory levels of human PC (hPC), a key factor in the potent anticoagulant protein C pathway, show a stable pattern with only marginal, if any, age-associated fluctuations [11,16,21]. Therefore, we considered that our studies on the age-related regulatory mechanisms of hFIX and hPC genes may provide us with critical information on the fundamental molecular mechanisms involved in the age-dimension homeostasis of gene expression.

Assay systems

Natural gene sizes of hFIX and hPC are approximately 40 and 13 kb pairs, respectively. To make experimental manipulations feasible, we constructed a series of their minigenes [26–31] (Fig. 2). After verifying with HepG2 cells for appropriate construction of these minigene vectors and their expression activities, all the minigene vectors were subjected to systematic

Correspondence: Kotoku Kurachi, Age Dimension Research Center, National Institute of Advanced Industrial Science and Technology, 1-1-1, Higashi, Tsukuba, Ibaraki, 305–8566, Japan.
Tel.: +81 298 61 6528; fax: +81 298 61 2788; e-mail: k.kurachi@aist.go.jp

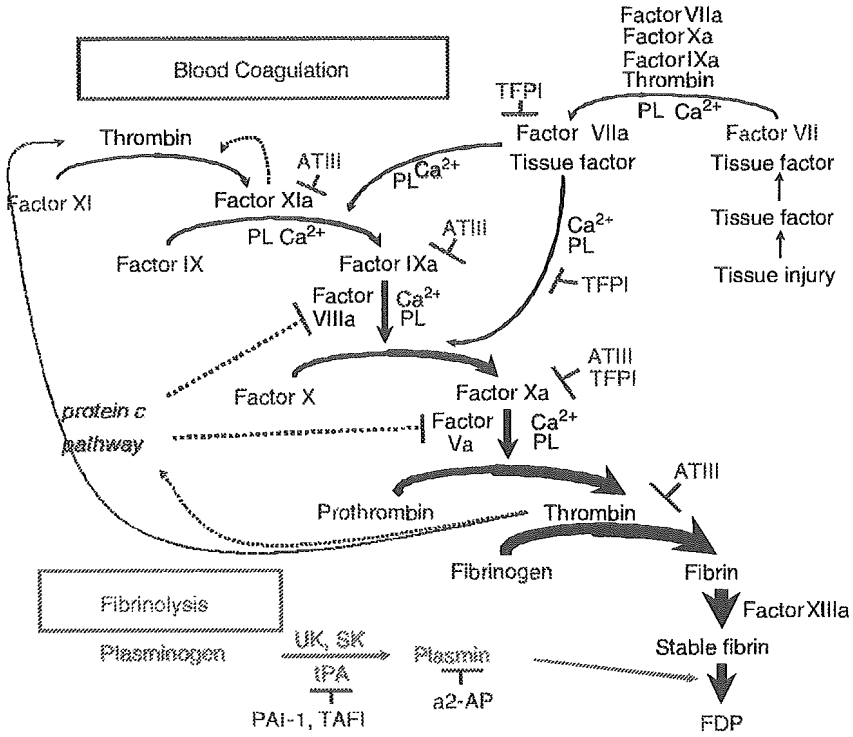

Fig. 1. Blood coagulation and fibrinolysis cascades. Procoagulation factors, shown with connecting arrows, increase their plasma concentrations or activities, while anticoagulation factors shown with T bars and profibrinolysis factors do not. Here, simplified blood coagulation and fibrinolysis cascades are shown to illustrate the essential relationships of factors involved.

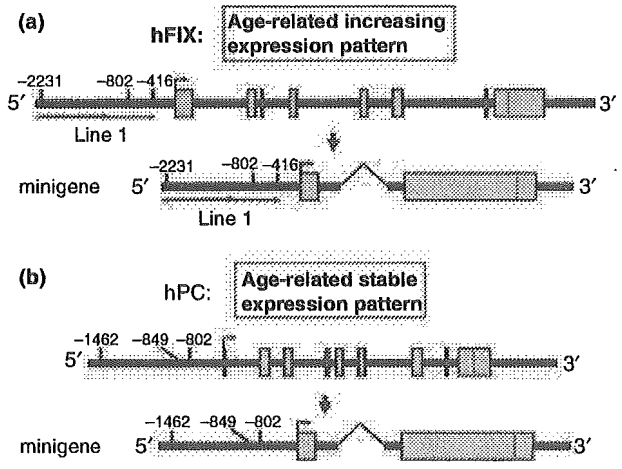

Fig. 2. Basic frameworks of minigene constructs of hFIX (a) and hPC (b) genes. hFIX and hPC genes are represented by horizontal lines with exons shown as fattened portions. Relative positions of LINE-1 (retrotransposable element)-derived sequences of the hFIX gene are shown with overlapped horizontal arrows. Exemplary minigenes are shown.

construction of transgenic mice. Circulatory levels of hFIX or hPC produced in individual transgenic animals were then monitored biweekly or monthly as needed for their life spans using serum samples and hFIX or hPC-specific enzyme-linked immunosorbent assays (ELISA).

Characteristics of the mouse blood coagulation system are similar to those of the human system, and we showed that age-related expression patterns of FIX and PC genes, age-related increase or stable, respectively, are also similar to those of the human counterparts [26,27]. This similarity justified mice as our animal model for analyzing the age-dimension homeostasis of gene expression.

Discovery of the first age-related regulatory mechanisms of gene expression

After systematic analyses of many lines of hFIX minigenes in transgenic mice, we identified two genetic elements, ASE and AIE (renamed from the initial names, AE5′- and AE3′, respectively; see [26,27]) to be essential for generating age-related stable and increase patterns, respectively, of hFIX gene expression [26] (Fig. 3). ASE is located to a small 5′ upstream region, nucleotide (nt) −802 to nt −784, of the hFIX gene sequence by footprinting assay and electrophoretic mobility shift assay (EMSA). ASE has a nucleotide core sequence, GAGGAAG, matching the Ets element consensus sequence (GGAAT) for the binding of Ets family transcriptional factors such as PEA-3 [32,33]. AIE, an element necessary for age-related increase in gene expression, was identified in the middle of the hFIX 3′-untranslated region (UTR) [26]. AIE is composed of a 102 base pair (bp) dinucleotide repeat (mostly AT, GT, CA), and has the potential to form three distinct stem loop structures in its RNA form [28]. Mouse factor IX (mFIX) shows an age-related increase in both its plasma level and gene expression level in the liver [34,35], and its gene contains an

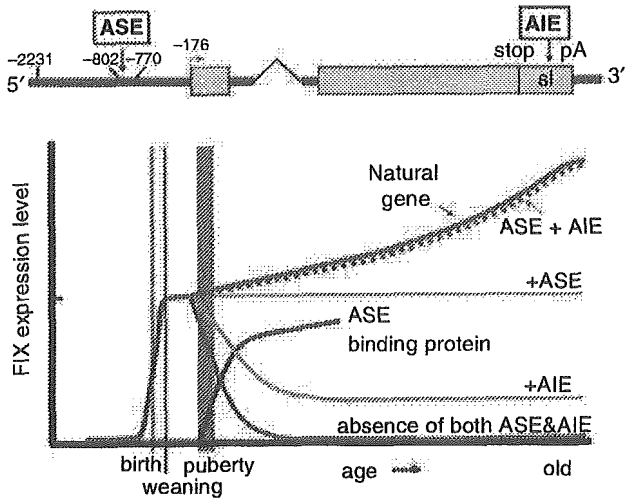

Fig. 3. The age-regulatory mechanisms of the hFIX gene. Relative positions of genetic components, ASE and AIE are shown at the top. Age-related patterns of circulatory hFIX levels for minigenes with or without ASE and/or AIE are shown schematically. These patterns are essentially parallel to those of the hFIX mRNA levels in the liver tissues.

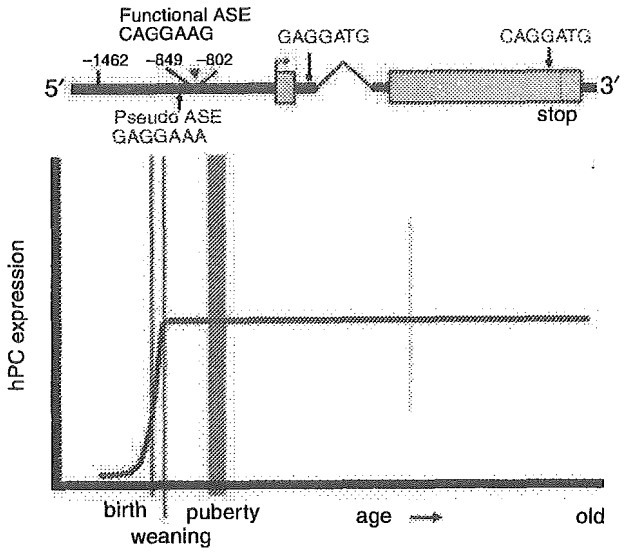

Fig. 4. Mechanisms of age-related regulation of the hPC gene. The age-stable expression pattern of the hPC gene due to the presence of its functional ASE (CAGGAAG) and absence of any AIE is shown in the lower panel. Relative positions of the similar Ets consensus sequences but with no age-regulatory function are also shown with thin letters.

ASE sequence identical to the functional ASE in the hFIX gene and an AIE-like stretch of 106 bp dinucleotide repeats in the mFIX 3′-UTR [36]. Through testing in transgenic mice, we showed that the mFIX repeat actually functions as an active AIE [27]. These studies demonstrated that the age-related increase in expression of the FIX gene is regulated by a combination of two unique genetic elements, ASE and AIE (Fig. 3). In the absence of ASE, minigenes with or without AIE show an age-unstable hFIX gene expression pattern with a rapid decline in expression over the puberty period, and in the subsequent 3–4 months decline to low but stable levels or very low basal levels, respectively. In the presence of both ASE and AIE, the age-related expression increase pattern of the hFIX gene is reproduced. Importantly, the clearance rate ($t_{½}$) of human factor IX from the blood circulation does not change significantly over age [26,27]. This is the first discovery of the age-related regulatory mechanisms of gene expression.

What molecular mechanisms function in regulation of age-stable hPC gene expression? As mentioned above, we first confirmed that the mouse PC gene expression pattern is age-stable, similar to that of the hPC gene [27]. hPC and hFIX share significant similarities in protein structure and therefore coding regions of their genes, whereas the 5′-flanking regions and 3′-UTRs are grossly dissimilar, indicating unrelated evolutional origins [28,30,37,38]. For example, we have shown previously that the 5′-flanking region of the hFIX gene beyond approximately nt −350, including the region containing ASE, was derived from the retrotransposable element LINE-1 inserted into the 5′ UTR [38] (Fig. 2). In contrast, the 5′-flanking region of the hPC gene has no LINE-1 or its remnant sequences, indicating that no retrotransposition events took place. In addition, 3′-UTR sequences of hFIX and hPC genes share no similarity except the minimal local sequences required for polyadenylation at the 3′ end regions. The 3′-UTR sequence of the hFIX gene is about 1.4 kb in length, whereas that of the hPC gene is only 295 bp, and has no AIE or AIE-like element or dinucleotide repeats [28,30]. These differences between the hFIX and hPC genes correlated with the dissimilarities in their age-related expression patterns as well as tissue-specific expression patterns.

As shown in Fig. 4, age-related stable patterns of circulatory hPC were observed with transgenic mice carrying hPC minigene −1462hPCm1 or −849hPCm1, recapitulating the natural age-stable expression patterns of mPC and hPC genes [27].

These minigenes had 5′ flanking sequences where their promoter regions are contained, extending to either nt −1462 or −849, respectively. However, expression patterns of minigene −802hPCm1 were age-unstable, thus identifying CAGGAAG, present in the region spanning nt −832 to nt −826, as the functional hPC ASE responsible for the age-stable expression pattern of the hPC gene. The functional ASE sequences of both hPC and hFIX genes bind the same liver nuclear protein, but other sequences do not function even with their close similarity, as shown by EMSA DNA-protein binding assays [27]. It is important to emphasize that hFIX ASE and hPC ASE have independent evolutionary origins. hFIX ASE was derived through mutational changes of a LINE-1 sequence inserted originally by a retrotransposition, while the hPC gene never experienced LINE-1 retrotransposition, and its ASE was derived through a different mechanism. This is a case of function-driven convergent evolution generating a critical genetic element required for homeostatic regulation of genes.

Pseudo-ASE (GAGGAAA) present at the 5′ upstream close to the functional hPC ASE binds a nuclear protein different